How to locate services optimizing redundancy: A comparative analysis of K-Covering Facility Location models

Socio-Economic Planning Sciences 94 (2024) 101938

Contents lists available at ScienceDirect

Socio-Economic Planning Sciences

journal homepage: www.elsevier.com/locate/seps

How to locate services optimizing redundancy: A comparative analysis of K-Covering Facility Location models

Edoardo Fadda [a], Daniele Manerba [b,*], Roberto Tadei [c]

[a] Department of Mathematical Sciences, Politecnico di Torino, Turin, Italy
[b] Department of Information Engineering, Università degli Studi di Brescia, Brescia, Italy
[c] Department of Control and Computer Engineering, Politecnico di Torino, Turin, Italy

ARTICLE INFO

Keywords:
Service redundancy
Backup-coverage problems
Double Standard Model
Ambulances location

ABSTRACT

Redundancy aspects related to covering facility location problems are of extreme importance for many applications, in particular those regarding critical services. For example, in the healthcare sector, facilities such as ambulances or first-aid centers must be located robustly against unpredictable events causing disruption or congestion. In this paper, we propose different modeling tools that explicitly address coverage redundancy for the underlying service. We also evaluate, both theoretically and experimentally, the properties and behavior of the models, and compare them from a computational and managerial point of view. More precisely, by starting from three classical double-covering models from the literature (BACOP1, BACOP2, and DSM), we define three parametric families of models (namely, K-BACOP1, K-BACOP2, and K-DSM) which generalize the former to any possible Kth coverage level of interest. The study of such generalizations allows us to derive interesting managerial insights on location decisions at the strategic level. The CPU performance and the quality of the solutions returned are assessed through ad-hoc KPIs collected over many representative instances with different sizes and topological characteristics, and also by dynamically simulating scenarios involving possible disruption for the located facilities. Finally, a real case study concerning ambulance service in Morocco is analyzed. The results show that, in general, K-BACOP1 performs very well, even if intrinsic feasibility issues limit its broad applicability. Instead, K-DSM achieves the best coverage and equity performances for lower levels of redundancy, while K-BACOP2 seems the most robust choice when high redundancy is required, showing smoother and more predictable trends.

1. Introduction

Facility location is a fundamental strategic and tactical aspect in many decision processes, with uncountable applications in logistics, transportation, healthcare, and many other fields [1–3]. In all these problems, the significant decisions to be taken are about locating facilities (where and how many) while making the underlying service as efficient as possible. In general, objectives can relate to topological, covering, equity, and accessibility aspects [4–7]. The *p-median*, *p-center*, or the *Simple Plant Location* problem are just a few well-known examples. Inside the class mentioned above, the so-called *covering location problems* (CLPs) are among the most important and adopted models [8]. Given the covering radius of each potential facility, the main goal of such problems is to locate facilities to cover the demand centers as best as possible in terms of service (i.e., so that they result in a reasonable amount of time or distance to the nearest located facility). They can be subdivided into two main groups, namely, *mandatory* and *maximal* CLPs. The former problems seek to minimize the number of facilities to cover all the demand. In contrast, the latter ones seek to maximize the total covered demand by locating a predefined number of facilities (representing a limited available budget to invest in the service).

In this paper, we focus on maximal CLPs and their extensions. In particular, we are interested in studying their behavior when multiple covering of the same demand is desirable, the so-called *service redundancy*. Problems that consider high multi-coverage levels are helpful for settings that require pursuing more sophisticated goals than the basic coverage, e.g., those related to the robustness or resiliency of the service. Given their critical impact on the population, healthcare services (e.g., ambulance location or relocation) are typical cases in which decision-makers (e.g., municipalities, healthcare companies, hospitals) must pay particular attention to the performance of the implemented solutions [9–11]. This is particularly true when possible disruption or congestion of the facilities is concerned. While healthcare applications have been studied long since from the redundancy point of view (see,

* Correspondence to: via Branze 38, 25123 Brescia, Italy.
E-mail addresses: edoardo.fadda@polito.it (E. Fadda), daniele.manerba@unibs.it (D. Manerba), roberto.tadei@formerfaculty.polito.it (R. Tadei).

https://doi.org/10.1016/j.seps.2024.101938
Received 15 May 2023; Received in revised form 2 April 2024; Accepted 18 May 2024
Available online 21 May 2024

e.g., [12]), this aspect has gained further importance during the SARS-CoV-2 pandemic. The location of triage or vaccine centers, ambulances, and outstanding intensive care facilities are just a few among several possible interesting cases of CLPs applications to deal with that kind of healthcare crisis. Apart from healthcare, many other services are particularly sensitive to redundancy features. For example, energetic facilities must be carefully located to be fault tolerant, while capacity-limited services (such as waste bins or parking areas) try to robustly meet the demand by enlarging its possibility to be satisfied by locating more covering facilities. Finally, even for services rarely affected by disruptions (such as schools, markets, or green areas) covering with redundancy is always preferred since it allows more and more different alternatives to choose from, thus increasing social inclusion and equal opportunities.

Facility disruption can be addressed under three main perspectives: Deterministic, stochastic (at the tactical level), and dynamic (at operational and real-time levels). The deterministic perspective considers planning models that ignore the decision process's intrinsic uncertainty. However, most covering facility location models can be solved optimally nowadays by state-of-the-art solvers, even for large instances. Clearly, basic covering problems cannot explicitly create robust solutions in the case of disruption related to already-located facilities. Instead, some tailored models are available in the literature as the *BAckup COverage Problem of type 1* (BACOP1), the *BAckup COverage Problem of type 2* (BACOP2) presented in Hogan and ReVelle [13], and the *Double Standard Model* (DSM) presented in Gendreau et al. [14]. All the models try to maximize, with some differences, the number of times a location is covered at least twice. This way, if a facility is disrupted, then a backup one can provide the same service to the demand center. On the contrary, the stochastic perspective explicitly considers that facilities operate in uncertain environments. Some quantities (e.g., the service demand or the probability of disruption) are unknown a-priori. Usually, such models are very complex to solve, and ad-hoc heuristics are needed. Moreover, these models are typically problem-specific and can hardly be adapted from one context to another one. Finally, at the operational and real-time levels, the dynamic perspective considers the problem of relocating facilities in an optimal way over a specific time horizon. Solutions for these problems are commonly computed by using heuristics based on dynamic programming concepts. These models are adopted in the presence of facilities that can be moved or reallocated (e.g., ambulances) or to address progressive location interventions over time. However, they do not provide robust solutions, and results are useless for many facilities (i.e., all those that cannot be reallocated).

The purpose of this paper is to study and compare insightful modeling tools able to assess redundancy aspects of facility location from many different perspectives at the strategic level. In fact, in many cases (e.g., during the exploratory phases of a decision process), the problem objectives are not very clear and the choice of the *right* model to use (together with its right parameterization) becomes of utmost importance and must be, therefore, supported by a quantitative analysis. A similar perspective has been adopted, e.g., in Klibi et al. [15], where the authors investigate various modeling features of the location–allocation model and compare location decisions produced by stochastic and deterministic models, or in Fadda et al. [16], where several deterministic covering location models are compared against a large battery of post-optimality KPIs. In particular, the contribution of this work is two-fold:

- We enrich the deterministic planning research stream by defining new families of parametric models (K-BACOP1, K-BACOP2, and K-DSM) which generalize the three models mentioned above concerning redundancy. These K-covering generalizations, while preserving the same spirit of their 2-covering counterpart, involve decisions up to the Kth level of coverage, i.e., the status of the demand centers covered at least K times. This allows the decision-maker to better deal with applications characterized by services of critical importance, thus pursuing robust solutions through redundant demand coverage. The proposed models give the decision-maker more flexible and powerful tools for deriving location solutions with the desired redundancy.
- We assess the proposed models both from a theoretical and an empirical perspective. More specifically, feasibility, structural, and complexity properties are explored and derived. We also experimentally compare the returned location solutions' quality using ad-hoc KPIs collected for many artificial instances (simulating several different topological distributions of the centers, covering radii, number of available facilities to locate) as well as for a real case study concerning ambulance service in Morocco. The experiments are run both with and without considering the possible dynamic disruption of the locations. The analysis allowed us to derive reliable insights into the different models' applicability within the various simulated situations and their pros and cons against specific KPIs developed to assess the equity and redundancy of the solutions. Note that the above KPI-based analysis is doable and consistent since, despite being different in terms of objectives and combinatorial structure, all the three families of models proposed share a central decisional core (i.e., the facilities' location).

We acknowledge that K-BACOP1 and K-BACOP2 models can be obtained as special cases of the parametric formulation called COV discussed in García and Marín [8]. Actually, K-BACOP2 is obtainable from COV only under the simplifying assumption for which covering the demand of each location k times is at least as important as covering it $k+1$ times. The K-DSM, instead, seems to have never appeared in the specialized literature. However, the COV model is too general and, therefore, potentially less efficient to solve than our formulations. Moreover, to the best of our knowledge, the proposed formulations have never been studied and analyzed in detail, nor adopted for specific applications. Finally, while our generalizations have not been studied in the literature for covering problems, similar extensions have been proposed for *p-median* and *p-center* models under the name of Fault-Tolerant Facility Location Problems [17–21].

The rest of the paper is organized as follows. In Section 2, we review the most relevant literature concerning covering location problems, emphasizing those addressing redundancy aspects. In Section 3, we present and discuss the three most used 2-covering models from the literature. Instead, in Section 4, we propose new parametric families of models generalizing the previous ones to any Kth level of desired coverage. Then, Section 5 explores some theoretical properties of the proposed models. Concerning the empirical comparison, Section 6 presents the experimental setting used to compare and evaluate the models, while Section 7 provides an insightful discussion on the results obtained over a large number of experiments. Section 8 presents the case study and the relative results. Finally, Section 9 concludes the paper and sketches possible future research.

2. Literature review

In this paper, we are interested in addressing maximal covering location problems (MCLPs) and their extensions [22]. As already said, MCLPs can be either deterministic or stochastic. Moreover, they can consider dynamic relocation when possible and be uncapacitated or include some capacity constraints.

For capacitated MCLPs, the service congestion or disruption must be explicitly addressed by taking care of coverage redundancy in the model. Classical models doing that are the Redundant Covering Location Problem (RCLP) [23], the Maximal Backup Coverage Location Problems (MBCLPs), in particular BACOP1 and BACOP2 [13], and the DSM [14]. The RCLP considers Minimum Set Covering Problem (MSCP) solutions that maximize the demand covered at least twice. In BACOP1, the total demand is assumed to be covered once, while

the demand covered twice is maximized. BACOP2 instead is a multi-objective problem that simultaneously maximizes the single and the double coverage for the demand. At the same time, no guarantee is given that all the demand is covered. Finally, in the DSM, two covering radii are considered, r_1 and r_2 (with $r_1 < r_2$). The total demand is covered within radius r_2, while the demand covered within radius r_1 is maximized. Note that all these models can only consider the second level of coverage (i.e., only one backup in the case of disruption). Still, they cannot provide robust solutions if the decision-maker is interested in higher levels of coverage. However, while BACOP-1 and BACOP-2 are binary problems, DSM is an integer problem. Extensions of DSM can be found in Doerner et al. [24],Doerner and Hartl [25] for the minimization of the ambulance workload.

Applications of deterministic MCLPs explicitly taking into account redundancy (e.g., MBCLP and DSM) are widely found in the emergency services location [26], the design of hierarchical healthcare systems [27,28], and the optimization of congested service systems [29]. In all these settings, the coverage criterion becomes strategic and highly critical. An excellent taxonomy of healthcare design is given by Ahmadi-Javid et al. [30]. Other interesting applications of those models can be found for the design of firefighting emergency systems [29] and police/military systems [31–33]. However, the following limit affects all the coverage models: An irrelevant distance difference moves a demand from covered to uncovered due to border effects. To address this issue, a two-threshold decay function has been introduced by Karasakal and Karasakal [34] and gradual deterministic models have been proposed by Berman et al. [35],Berman and Wang [36], and Drezner et al. [37]. An interesting review of this topic can be found in Eiselt and Marianov [38].

The most used techniques to solve MCLP, MBCLP, and DSM are exact methods, mainly relying on Benders-like decomposition [39] or Dynamic Programming [40]. Despite their theoretical complexity, such models can be solved optimally in a reasonable amount of time by state-of-the-art solvers or ad-hoc procedures, even for large instances. However, many heuristics are also available in the literature, in particular for the most complicated extensions. Lagrangian relaxation-based heuristics can be found in Karasakal and Karasakal [34],Galvão and ReVelle [41] for the MCLP and its partial coverage version, respectively. Gendreau et al. [42,43] use tabu search for ambulances relocation, while Doerner et al. [24] develop a tabu search method to solve the DSM for instances representing ambulance location in Austria. An interesting survey on covering models and optimization techniques for emergency response facility location can be found in Li et al. [44].

Concerning stochastic MCLPs, several sources of uncertainty characterize these models: Demand, service availability, and response time. Demand uncertainty is addressed by Sung and Lee [45],MirHassani et al. [46]. Stochastic service availability is introduced by ReVelle and Hogan [47],Daskin [48], through the Maximum Expected Covering Location Problem (MEXCLP). Sorensen and Church [49] integrate the contributions of ReVelle and Hogan [47],Daskin [48] by considering a reliable MEXCLP, while Rajagopalan et al. [50] introduce genetic algorithms for solving the MEXCLP. Stochastic response time is addressed by Chelst and Jarvis [51] by introducing the probability distribution of travel times. Drezner et al. [52] give a random gradual covering problem, while Drakulic et al. [53] consider fuzzy coverage radii and distances. Stochastic models are also introduced to address capacitated facility locations' reliability to guarantee a minimum service level under facility disruptions (see, e.g., [54–59], and [60]). Most of them are stochastic versions of the classical Uncapacitated Fixed-charge Location Problem (UFLP) or of the Capacitated Fixed-charge Location Problem (CFLP). The uncertainty is generally modeled through a scenario-based approach. When two-stage Stochastic Programming models are developed, the number and location of the facilities are determined in the first stage. In contrast, in the second stage, after uncertainty due to disruptions is resolved, the allocation of users to facilities is calculated for each disruptive scenario. Robust and distributionally robust approaches have also been investigated (see, e.g., [61,62], and [63]). For extended reviews on facility location under disruption, see Snyder et al. [64],Scaparra and Church [65].

Concerning the dynamic setting, we just point out that, in Dibene et al. [66], the authors adopt a DSM by also considering a dynamic service demand. The relocation of facilities, which is another way to address dynamic demand, is considered by Brotcorne et al. [12],Gendreau et al. [43],Carson and Batta [67],Moeini et al. [68], and Bélanger et al. [69].

3. Double-covering models

This section presents and discusses the three most-used existing models, namely the BACOP1, BACOP2, and the DSM, which address redundancy by explicitly introducing a double level of service coverage. Given their wider generality, we will consider weighted versions of such models, i.e., where possibly different weights (demand rates) are associated with each location. In particular, BACOP1 pursues the maximization of the demand rate related to the locations covered twice, while BACOP2 maximizes the convex combination of the demand rate related to the locations covered once and twice. Finally, DSM pursues the same objective of BACOP1 but, considering two different coverage radii, it enforces the covering of all facilities within the largest radius and a certain percentage of demand rate covered within the smallest one. Let us consider the following notation:

- $\mathcal{N}$: Set of locations where it is possible to locate a facility for the considered service;
- $h_i > 0$: Demand rate associated with location $i \in \mathcal{N}$;
- d_{ij}: Distance between locations $i, j \in \mathcal{N}$;
- $C_i^r = \{j \in \mathcal{N} : d_{ij} \leq r\}$: Covering set of $i \in \mathcal{N}$, i.e., the set of all locations closer to location i than a predefined radius r. The value of r could represent, e.g., the maximum distance that a user is willing to drive to reach a facility;
- $r_1 > 0, r_2 > 0$: Inner and outer coverage radius, respectively (we assume $r_2 > r_1$). While r_1 is used to measure the backup coverage in all three models, r_2 is used only by DSM for ensuring a complete single covering of the service;
- p: Predefined number of facilities to locate (we assume $1 \leq p \leq |\mathcal{N}|$).

Moreover, let us consider the following common decision variables:

- y_j: Binary variable taking value 1 if a facility is located in $j \in \mathcal{N}$, and 0 otherwise;
- $u_i^{(1)}$, $u_i^{(2)}$: Binary variable taking value 1 if the demand from location $i \in \mathcal{N}$ is covered at least once and twice within r_1, respectively.

The BACOP1, presented in Hogan and ReVelle [13], is:

$$\max \quad \sum_{i \in \mathcal{N}} h_i u_i^{(2)} \tag{1}$$

$$\text{s.t.} \quad \sum_{i \in \mathcal{N}} y_i = p \tag{2}$$

$$u_i^{(2)} + 1 \leq \sum_{j \in C_i^{r_1}} y_j, \qquad \forall i \in \mathcal{N} \tag{3}$$

$$y_i, u_i^{(2)} \in \{0, 1\}, \qquad \forall i \in \mathcal{N}. \tag{4}$$

The objective function (1) aims at maximizing the total demand rate of the locations that are covered twice. Constraint (2) ensures to locate exactly p stations while constraints (3) ensure that $u_i^{(2)} = 0$ when location i is not covered by more than one facility in $C_i^{r_1}$. Note that BACOP1 returns feasible solutions only if there are enough facilities to cover all the locations once. It is easy to see that constraints (3) cannot be satisfied when their right-hand sides are strictly less than 1.

The BACOP2, presented in Hogan and ReVelle [13], is:

$$\max \quad \lambda^{(2)} \sum_{i\in\mathcal{N}} h_i u_i^{(2)} + \lambda^{(1)} \sum_{i\in\mathcal{N}} h_i u_i^{(1)} \tag{5}$$

$$\text{s.t.} \quad \sum_{i\in\mathcal{N}} y_i = p \tag{6}$$

$$u_i^{(2)} \le u_i^{(1)}, \qquad \forall i \in \mathcal{N} \tag{7}$$

$$u_i^{(2)} + u_i^{(1)} \le \sum_{j\in C_i^{r_1}} y_j, \qquad \forall i \in \mathcal{N} \tag{8}$$

$$y_i, u_i^{(1)}, u_i^{(2)} \in \{0,1\}, \qquad \forall i \in \mathcal{N} \tag{9}$$

where $\lambda^{(1)}$ and $\lambda^{(2)}$ are the relative importance of the single and the double coverage, respectively, with $\lambda^{(1)}, \lambda^{(2)} \ge 0$ and $\lambda^{(1)} + \lambda^{(2)} = 1$. Basically, the objective function (5) aims at maximizing a convex combination (weighted by $\lambda^{(1)}$ and $\lambda^{(2)}$) of the total demand rate of the locations covered once and twice, thus pursuing a trade-off between basic and backup coverage.[1] Constraints (7) enforce that if a location is covered at least two times, then it is also covered at least once. Constraints (8) ensure that the sum $u_i^{(2)}+u_i^{(1)}$ cannot exceed the number of times that location i is covered by facilities in $C_i^{r_1}$. This means that if $u_i^{(2)} = 1$, then also $u_i^{(1)} = 1$ and therefore the number of covering facilities must be greater than or equal to 2, while if $u_i^{(1)} = 1$, the number of covering facilities must be greater than or equal to 1.

Finally, the DSM, presented in Gendreau et al. [14], is[2]:

$$\max \quad \sum_{i\in\mathcal{N}} h_i u_i^{(2)} \tag{10}$$

$$\text{s.t.} \quad \sum_{i\in\mathcal{N}} y_i = p \tag{11}$$

$$\sum_{j\in C_i^{r_2}} y_j \ge 1, \qquad \forall i \in \mathcal{N} \tag{12}$$

$$\sum_{i\in\mathcal{N}} h_i u_i^{(1)} \ge \alpha^{(1)} \tag{13}$$

$$u_i^{(2)} \le u_i^{(1)}, \qquad \forall i \in \mathcal{N} \tag{14}$$

$$u_i^{(1)} + u_i^{(2)} \le \sum_{j\in C_i^{r_1}} y_j, \qquad \forall i \in \mathcal{N} \tag{15}$$

$$y_i, u_i^{(1)}, u_i^{(2)} \in \{0,1\}, \qquad \forall i \in \mathcal{N} \tag{16}$$

where $\alpha^{(1)}$ is the proportion of demand that must be covered at least once within r_1. The objective function (10) aims at maximizing the total demand rate of locations covered at least twice within r_1. Constraints (12) state that all demand must be covered within r_2, while constraints (13) ensure that a certain proportion of all demand is covered within r_1. Constraints (14) and (15), similarly to constraints (7) and (8) for the BACOP2, express the double coverage requirement within r_1.

4. *K*-covering models

In this section, we generalize the three models previously presented to any possible coverage level. To this aim, we need to further define:

- K: Maximum level of coverage desired. Obviously, this value cannot exceed the available number of facilities to locate, i.e. $K \le p$;
- $u_i^{(k)}$: Binary variable taking value 1 if the demand from location $i \in \mathcal{N}$ is covered at least k times (with $k = 1, \dots, K$) within r_1, and 0 otherwise.

Each of the following subsections is dedicated to a specific model generalization.

4.1. *K-BACOP1*

The proposed generalization to the Kth level of coverage of BACOP1 (K-BACOP1) is as follows:

$$\max \quad \sum_{i\in\mathcal{N}} h_i u_i^{(K)} \tag{17}$$

$$\text{s.t.} \quad \sum_{i\in\mathcal{N}} y_i = p \tag{18}$$

$$u_i^{(K)} + K - 1 \le \sum_{j\in C_i^{r_1}} y_j, \qquad \forall i \in \mathcal{N} \tag{19}$$

$$y_i \in \{0,1\}, \qquad \forall i \in \mathcal{N} \tag{20}$$

$$u_i^{(K)} \in \{0,1\}, \qquad \forall i \in \mathcal{N}. \tag{21}$$

As in the BACOP1, the objective function (17) aims at maximizing the total demand rate of the locations covered at the maximum level considered, i.e. K. Along with the usual budget constraint (18), constraints (19) generalize constraints (3) to the Kth covering level, i.e., they ensure that $u_i^{(K)} = 0$ when location i is not covered by more than $K-1$ facilities in $C_i^{r_1}$. Clearly, the model is equivalent to the BACOP1 for $K = 2$. Finally, as already mentioned in the Introduction, the K-BACOP1 can be seen as a special case of the general model called COV presented in García and Marín [8].

4.2. *K-BACOP2*

The proposed generalization to the Kth level of coverage of BACOP2 (K-BACOP2) is as follows:

$$\max \quad \sum_{k=1}^{K} \lambda^{(k)} \sum_{i\in\mathcal{N}} h_i u_i^{(k)} \tag{22}$$

$$\text{s.t.} \quad \sum_{i\in\mathcal{N}} y_i = p \tag{23}$$

$$u_i^{(k)} \le u_i^{(k-1)}, \qquad \forall i \in \mathcal{N}, \forall k = 2, \dots, K \tag{24}$$

$$\sum_{k=1}^{K} u_i^{(k)} \le \sum_{j\in C_i^{r_1}} y_j, \qquad \forall i \in \mathcal{N} \tag{25}$$

$$y_i \in \{0,1\}, \qquad \forall i \in \mathcal{N} \tag{26}$$

$$u_i^{(k)} \in \{0,1\}, \qquad \forall i \in \mathcal{N}, \forall k = 1, \dots, K \tag{27}$$

where $\lambda^{(k)}$ is the relative importance of the kth coverage, with $\lambda^{(k)} \ge 0$ and $\sum_{k=1}^{K} \lambda^{(k)} = 1$.

Basically, the objective function (22) aims at maximizing a convex combination, weighted by $\lambda^{(k)}$, of the demand rate of the locations covered k times. Along with the budget constraint (23), constraints (24) generalize constraints (7) by enforcing that a location covered k times must also be covered $k-1$ times, while constraints (25) generalize constraints (8) ensuring that the sum of all the u variables related to location i cannot exceed the number of times i is covered by facilities in $C_i^{r_1}$. Clearly, the model is equivalent to the BACOP2 for $K = 2$. Again, the K-BACOP2 can be seen as a special case of the COV model. However, COV does not explicitly include the constraints (24) whereas it requires a particular assumption on the objective function's coefficients ensuring that it is never convenient to cover k times a location without having covered it $k-1$ times.

4.3. *K-DSM*

The proposed generalization to the Kth level of coverage of DSM (K-DSM) is as follows:

[1] Actually, BACOP2 was born as a pure multi-objective problem. However, to maintain uniformity with the other problems and as commonly done in the literature [70–72], we stick with a formulation in which the objective function has been linearized.

[2] In the original DSM version, which concerned ambulances location, decision variables might take integer values and not merely binary ones. However, to maintain a sensible comparison with the other models, we consider a binary DSM version. This does not affect the model's main characteristics and the essence of its location goals.

$$\max \quad \sum_{i\in\mathcal{N}} h_i u_i^{(K)} \tag{28}$$

$$\text{s.t.} \quad \sum_{i\in\mathcal{N}} y_i = p \tag{29}$$

$$\sum_{j\in C_i^{r_2}} y_j \geq 1, \qquad \forall i \in \mathcal{N} \tag{30}$$

$$\sum_{i\in\mathcal{N}} h_i u_i^{(k)} \geq \alpha^{(k)}, \qquad \forall k = 1,\dots,K-1 \tag{31}$$

$$u_i^{(k)} \leq u_i^{(k-1)}, \qquad \forall i \in \mathcal{N}, \forall k = 2,\dots,K \tag{32}$$

$$\sum_{k=1}^{K} u_i^{(k)} \leq \sum_{j\in C_i^{r_1}} y_j, \qquad \forall i \in \mathcal{N} \tag{33}$$

$$y_i \in \{0,1\}, \qquad \forall i \in \mathcal{N} \tag{34}$$

$$u_i^{(k)} \in \{0,1\}, \qquad \forall i \in \mathcal{N}, \forall k = 1,\dots,K \tag{35}$$

where $\alpha^{(k)}, \forall k = 1,\dots,K-1$ is the proportion of demand that must be covered at least k times within r_1.

The objective function (28) maximizes the demand covered at least K times. Along with constraints (29) and (30), which are identical to (11) and (12), constraints (31) enforce a minimum percentage of h_i covered at least k times, generalizing (13). Finally, constraints (32) and (33) link the u and y variables exactly as in the K-BACOP2, generalizing (14) and (15), respectively.[3] Clearly, the model is equivalent to the DSM for $K = 2$.

5. Theoretical properties

In this section, we compare K-BACOP1, K-BACOP2, and K-DSM from a theoretical point of view by exploring some interesting mathematical properties. Some of these properties will be useful to fully grasp the experimental results presented in Section 7. In the following, we call K-DSM$_r$ the K-DSM problem in which constraints (31) are relaxed.

5.1. Complexity

All the proposed problems are $\mathcal{NP}$-hard, being generalizations of the well-known Maximal Covering Problem (MCP). In fact, K-BACOP1 is equivalent to MCP for $K = 1$ while K-BACOP1 is a particular case of K-BACOP2 where $\lambda^{(K)} = 1$ and reduced by fixing $u_i^{(k)} = 1$, $k = 1,\dots,K-1$. Finally, K-BACOP2 is a particular case of K-DSM in which $\lambda^{(K)} = 1$ and where constraints (30) and (31) are relaxed. Notice that, as it happens for many classical covering problems (e.g., the MCP), some particular cases may be easy to solve. For instance, when $p = |\mathcal{N}|$ then the optimal solution can be obtained by simply locating all the facilities, or when each facility covers only the location where it is located (i.e., $C_i^r = \{i\}, \forall i \in \mathcal{N}$), then the optimal solution can be obtained by simply locating a facility in the p locations with the largest demand rate.

5.2. Dimensionality

Apart from the theoretical complexity, which is the same for the three proposed models, it is also interesting to compare them in terms of the number and type of variables and constraints required. In fact, such aspects generally affect computational performances in practice.

First, it is interesting to notice that some variables can be relaxed to be continuous without changing the solution of the models. In particular:

[3] Another reasonable DSM generalization may consider K different radii, one for each coverage level. However, such a generalization would deny a direct comparison with the other proposed models.

Table 1
Number of variables and constraints of the models.

	K-BACOP1	K-BACOP2	K-DSM
Binary variables	$\lvert\mathcal{N}\rvert$	$(K+1)\cdot\lvert\mathcal{N}\rvert$	$(K+1)\cdot\lvert\mathcal{N}\rvert$
Continuous variables	$\lvert\mathcal{N}\rvert$	0	0
Constraints	$\lvert\mathcal{N}\rvert+1$	$K\cdot\lvert\mathcal{N}\rvert+1$	$(K+1)\cdot\lvert\mathcal{N}\rvert+K$

Property 1. *Given K, all the variables u_i^K, $\forall i \in \mathcal{N}$, can be relaxed to be continuous in the K-BACOP1.*

In fact, Eq. (19) impose an integer upper bound on each $u_i^{(K)}$, and, therefore, in the case this bound is greater than 1, then the objective function pushes each $u_i^{(K)}$ to take the maximum value in $[0,1]$.

Property 2. *Given K, all the variables u_i^k, $\forall i \in \mathcal{N}, \forall k = 1,\dots,K$, can be relaxed to be continuous in the K-BACOP2, when $\lambda^{(k)} < \lambda^{(k-1)}, \forall k = 2,\dots,K$.*

Property 3. *Given K, all the variables u_i^k, $\forall i \in \mathcal{N}, \forall k = 1,\dots,K$, can be relaxed to be continuous in the K-DSM$_r$.*

Concerning the K-BACOP2, the same observation done for K-BACOP1 holds for each level of coverage $k = 1,\dots,K$ only if it is always more convenient to cover a location k times than $k+1$ times, i.e., when $\lambda^{(k)} < \lambda^{(k-1)}, \forall k = 2,\dots,K$. Moreover, for a K-DSM with constraints (31) relaxed, the objective function pushes each $u_i^{(K)}$ to take the maximum value in $[0,1]$ by following the same logic described for K-BACOP2.

Then, a detailed comparison of the models in terms of the number of variables and constraints is reported in Table 1 (this analysis is based also on the consequences of Property 1, which does not need additional assumptions). The most interesting thing to notice is that, differently from the other two models, the dimension of K-BACOP1 does not depend on K. In fact, K-BACOP1, focuses only on the maximum desired level of coverage, while the intermediate levels are not considered (as it happens instead for K-BACOP2 and K-DSM). Considering the number of variables, K-BACOP2 and K-DSM both require $(K+1)\cdot|\mathcal{N}|$ binary variables, while K-BACOP1 requires only $2\cdot|\mathcal{N}|$ variables, half of which can be relaxed to be continuous. Considering the number of constraints, K-BACOP1 requires the smallest number, while the number of K-DSM constraints grows a little faster than that of K-BACOP2 as K increases.

5.3. Feasibility properties

We now explore the behavior of the three models in terms of feasibility with respect to the main input parameters, namely K, p, r_1, and r_2 (actually, r_2 is used only for the K-DSM). We remind that $K \leq p \leq |\mathcal{N}|$ is assumed throughout the paper. First, note that K-BACOP2 returns a feasible solution for any (K,p,r_1) combination. Instead, both K-BACOP1 and K-DSM suffer from possible infeasibilities. This is further explained through the following properties.

Concerning K-BACOP1, given a certain coverage level K, the model can be infeasible for any possible value of p depending on how small r_1 is. For instance, a r_1 value allowing each location to cover just itself yields a K-BACOP1 infeasible $\forall K \geq 2$ even when $p = |\mathcal{N}|$. More interesting:

Property 4. *If K-BACOP1 is infeasible for a given (K,p,r_1), then it is also infeasible for:*

- *$(K,\bar{p},r_1)$, with $\bar{p} < p$;*
- *$(K,p,\bar{r}_1)$, with $\bar{r}_1 < r_1$.*

A stronger implication can be derived concerning K-BACOP1 infeasibility with respect to the value of K:

Property 5. *Given (K,p,r_1) with $K \geq 2$, K-BACOP1 returns a feasible solution if and only if all the locations are covered at least $K-1$ times.*

This highlights the importance, for a given (K, r_1), to estimate the minimum number $p_{min}^{K\text{-BACOP1}}$ of facilities needed to cover $K-1$ times all the locations, and thus making feasible the K-BACOP1. The following *set* $(K-1)$*-covering problem* [73] returns such a threshold:

$$p_{min}^{K\text{-BACOP1}} = \min \sum_{i \in \mathcal{N}} y_i \tag{36}$$

$$\text{s.t.} \sum_{j \in C_i^{r_1}} y_j \geq K-1, \qquad \forall i \in \mathcal{N} \tag{37}$$

$$y_i \in \{0,1\}, \qquad \forall i \in \mathcal{N}. \tag{38}$$

Concerning K-DSM, the model can be infeasible due to constraints (30) and (31). For instance, if p is low and there exists a location placed at a distance greater than r_2, then the relative constraints (30) cannot be satisfied. Furthermore, according to constraints (31), there could exist characteristic values of $\alpha^{(k)}$ such that the model is infeasible even for $p = |\mathcal{N}|$. Hence, to derive some interesting properties, we need to assume that the $\alpha^{(k)}$ values do not affect the feasibility of the problem, i.e. to consider K-DSM$_r$ instead of K-DSM. Note that, although not general, this is reasonably true in practical applications, especially when the value of K grows. So, the following property holds:

Property 6. *If K-DSM$_r$ is infeasible for a given (K, p, r_1, r_2), then it is also infeasible for:*

- $(K, \bar{p}, r_1, r_2)$, *with* $\bar{p} < p$;
- $(K, p, \bar{r}_1, r_2)$, *with* $\bar{r}_1 < r_1$;
- $(K, p, r_1, \bar{r}_2)$, *with* $\bar{r}_2 < r_2$.

As before, for practical purposes, it is important to estimate the minimum number $p_{min}^{K\text{-DSM}_r}$ of facilities needed to make feasible the K-DSM$_r$ for a given (K, r_1, r_2). This value can be found by solving the following set-covering problem:

$$p_{min}^{K\text{-DSM}_r} = \min \sum_{i \in \mathcal{N}} y_i \tag{39}$$

$$\text{s.t.} \sum_{j \in C_i^{r_2}} y_j \geq 1, \qquad \forall i \in \mathcal{N} \tag{40}$$

$$y_i \in \{0,1\}, \qquad \forall i \in \mathcal{N}. \tag{41}$$

Instead, it is not possible to find easily the minimum number $p_{min}^{K\text{-DSM}}$ of facilities making feasible the original K-DSM, unless resorting to a problem as complex as the K-DSM itself. However, $p_{min}^{K\text{-DSM}_r}$ represents a useful lower bound for $p_{min}^{K\text{-DSM}}$.

6. Experimental setting for models assessment

While the core decisions of the proposed models remain the same (i.e., the location of the available facilities), their comparison is not straightforward since they pursue different objectives and requisites. Hence, to assess their behavior, we analyze their optimal solutions against some redundancy-focused performance indicators over an extensive set of random instances simulating different topological and demographic aspects. The generation of such instances is presented in Section 6.1, while the considered KPIs are presented in Section 6.2. For a more solid assessment, we evaluate the KPIs both (i) by assuming a static planning scenario and (ii) by simulating possible disruption of the facilities already located. Such a simulation is described in Section 6.3.

6.1. Instances generation

We generate a broad set of random instances representing realistic scenarios by adopting the method proposed in Fadda et al. [16] since it has proven to be a reliable method for exploring the properties of the solutions. However, our generation is enriched by the specific data necessary for the considered models and their generalization. We specify that all the data and the instance parameters are maintained proportional to derive insights not depending on the absolute values of parameters.

Each considered location is characterized by a demand and a spatial position. For each location $i \in \mathcal{N}$, a demand Q_i is drawn randomly in $[0, Q_{max}]$, then the demand rate h_i is obtained by normalizing the vector of the demands, i.e., $h_i = Q_i / \sum_{j \in \mathcal{N}} Q_j$. Note that, since all the models and the KPIs are based only on the demand rate, the absolute values of Q_i and Q_{max} do not influence the following analysis. Instead, the locations' position is generated by using different probability distributions within a $[-10, 10] \times [-10, 10]$ square. By changing the distribution used and its parameters, we can mimic specific demographic features and service demand dispersion. In particular, we consider three topologies with the following features:

- **mono-polar**: This topology simulates the case of a region where a single main cluster of locations exists, in addition to a few sparse locations around it (e.g., a district where there exists only one large city surrounded by tiny satellite municipalities). The coordinates of 80% of the location are drawn from a *Student's t* distribution with 3 degrees of freedom. Instead, the coordinates of the remaining 20% are drawn from a *Uniform* distribution.
- **multi-polar**: This topology simulates the case of a region where there exist several dispersed clusters of locations (e.g., a district with small-medium cities of similar sizes). The locations' coordinates are drawn from a sum of independent *Multinomial* distributions with random mean value and a unitary standard deviation.
- **uniform**: This topology simulates the case of a region where there are no clear clusters of locations, as they are all dispersed (e.g., an urban area where the demand is spread uniformly across the considered region). The coordinates of the locations are drawn randomly from a *Uniform* distribution.

At the end, d_{ij} is calculated as the Euclidean distance between each pair of locations $i, j \in \mathcal{N}$. This guarantees that the triangular inequality holds for the distances.

To simulate different budget conditions, we set the number of available facilities to locate as a certain fraction γ of the total number of locations, i.e., $p = |\mathcal{N}| \cdot \gamma$. We will consider values of γ between 0.1 and 0.9, with a 0.1 step. Furthermore, we generate the covering radii by setting two parameters μ_1 and μ_2 such that r_1 and r_2 represent the μ_1-th and the μ_2-th percentile of the empirical distribution of the distances, respectively. While only μ_1 is used for K-BACOP1 and K-BACOP2, both values are needed to define K-DSM. In particular:

- Concerning the inner radius r_1, we consider $\mu_1 = \{0.1, 0.2, 0.3\}$. Values greater than 0.3 would lead to too wide service coverage, thus generating trivial problems in which all the demand is covered several times even by locating very few facilities. Instead, values smaller than 0.1 would lead to problems for which a feasible solution exists only for too small values of K.
- Concerning the outer radius r_2, the value of μ_2 must be chosen greater than the value of μ_1. In several applications, μ_2 could be reasonably the double (or more)[4] of μ_1. However, since we want to test our models against more general conditions, we will consider not a single proportion but several combinations of values.

Finally, anytime a specific K-covering model is considered, additional parameters are needed, namely, $\lambda^{(k)}, \forall k = 1, \dots, K$, and $\alpha^{(k)}, \forall k = 1, \dots, K-1$. The parameters $\lambda^{(k)}$ weight the contribution of the various levels of coverage in K-BACOP2 models. We assume that $\lambda^{(k)}$ is

[4] In Gendreau et al. [14], the authors set $r_1 = 7$ minutes and $r_2 = 15$ minutes in applying the DSM to a use case related to ambulances location. The same has been done in several other papers. This can be used as a guideline for deciding the proportion between the two radii.

decreasing when k increases, i.e., we enforce that covering once is more important than covering twice, and so on. More precisely, we first calculate $\lambda^{(k)} = \frac{1}{k}, \forall k = 1, \dots, K$, then we normalize such values to obtain a real convex combination in the K-BACOP2 objective function. The parameters $\alpha^{(k)}$, instead, force the fraction of demand that must be covered in constraints (31) for K-DSM. We set $\alpha^{(k)} = 0.5 \cdot 10^{-k}, \forall k = 1, \dots, K-1$, so that the rapid decay to zero of the $\alpha^{(k)}$ coefficients and our generation of the h_i force the model to cover half of the demand with the first level of coverage. Then, for each other level $k > 1$, just one covered location is enough to satisfy the relative constraints. This mild choice has been made to avoid as much as possible infeasibility issues for K-DSM. In fact, this allows us to solve K-DSM$_r$ without excluding any feasible solution for the K-DSM.

6.2. KPI-based analysis

Comparing families of covering models with different objective functions may seem to be pointless. Instead, at a strategic level or during the exploratory phases of a decision process, selecting the suitable location model to use is a difficult task in itself, which an appropriate quantitative analysis should support. In fact, in real settings, all the requirements and factors to include inside the optimization process are often not completely clear (due to externalities, uncertainty, etc.) and several incomparable objectives (conflicting interests of different stakeholders) should be considered. For these reasons, we resort to assessing the models for some tailored KPIs that depend on the common structure of the returned solutions.

Given a solution of any of the presented models, let $\mathcal{L}_i$ be the set of locations closer than r_1 to location $i \in \mathcal{N}$ where a facility has been located, i.e., $\mathcal{L}_i = \{j \in C_i^{r_1} : y_j = 1\}$. First, we consider two important indicators proposed in Fadda et al. [16]:

- *weighted average coverage*, which represents the average of the demand rate covered, defined as

$$avgC := \frac{1}{|\mathcal{N}|} \sum_{i \in \mathcal{N}} h_i |\mathcal{L}_i|; \tag{42}$$

- *standard deviation of the redundant coverage*, which represents the standard deviation of the number of times each location is covered, defined as

$$stdC := \sqrt{\frac{1}{|\mathcal{N}|} \sum_{i \in \mathcal{N}} \left(|\mathcal{L}_i| - \frac{1}{|\mathcal{N}|} \sum_{i \in \mathcal{N}} |\mathcal{L}_i| \right)^2}. \tag{43}$$

While $avgC$ is a classical KPI measuring the service coverage on average over all the demand, $stdC$ is a measure of the coverage equity. In particular, the higher the standard deviation, the higher the difference in redundant coverage between different locations, and the lower the equity of the service coverage.

Moreover, we propose a family of k-parametric KPIs for specifically assessing the quality of the redundancy provided by a location plan, namely, the *weight of the kth coverage*, which represents the overall demand rate of those locations covered at least k times, and defined as

$$C(k) := \sum_{i \in \mathcal{N} : |\mathcal{L}_i| \geq k} h_i, \quad k = 1, 2, \dots, |\mathcal{N}|. \tag{44}$$

Note that, even if $C(k)$ is potentially defined for levels of coverage up to the number of locations $|\mathcal{N}|$, each instance could reveal, depending on the p value, a threshold $\bar{k} < |\mathcal{N}|$ for which $C(k) = 0, \forall k > \bar{k}$.

6.3. Disruption simulation

To assess the robustness of the proposed models' solutions against possible disruption of the located facilities, we simulate a disruption event for the instances already presented in Section 6.1 and calculate the KPI of interest before and after such an event. The *degree of disruption* of each simulated event is defined by a parameter $\varepsilon \in [0, 1]$ representing the fraction of the p facilities that become unavailable, so $\lfloor \varepsilon \cdot p \rfloor$ facilities are randomly removed from the solution.[5] In our experiments, we consider values of $\varepsilon \in [0, 0.75]$, with a 0.05 step, so that the two extremes give rise to scenarios with no disruption and very high disruption, respectively. To have statistically significant results against the random removal disruption event, we run 100 different repetitions and calculate the average for each considered indicator and each tested instance.

Finally, in these simulations, we need to consider the models' possible infeasibility in a more sophisticated way. While it makes sense to assess the models in static scenarios (Section 7.2.1) even when they do not return feasible solutions, a disruption simulation process without a feasible location solution is meaningless. So, we need to consider only combinations of values for p and K that always guarantee the instance feasibility for K-BACOP1 and K-DSM. Thus, given K, we consider values of p greater than

$$p_{min} := \max \left\{ p_{min}^{K\text{-BACOP1}}, p_{min}^{K\text{-DSM}_r} \right\},$$

which can be calculated using the already presented models (36)–(38) and (39)–(41), respectively.

7. Results and discussion

In the following, we report and analyze the results obtained from our experimental campaign over the artificial instances. Section 7.1 compares the model in terms of computational time and properties of the LP relaxation, while Section 7.2 focuses on the KPI-based analysis. Gurobi v9.1.1 solves all the models via its Python3 APIs. All the tests have been done on an *Intel(R) Core(TM)* i7-5500U CPU@2.40 GHz computer with 16 GB of RAM and running *Ubuntu* v20.04.

7.1. Computational comparison

In the following, we analyze the computational times of the proposed models concerning some of the characteristics of the instances. The main results are shown in Fig. 1, in a logarithmic scale. Here, each bar represents the average CPU time in seconds for solving one of the three models over 10 randomly generated instances for each combination of budget γ and coverage radii (μ_1, μ_2). Data are grouped per topology (mono-polar, multi-polar, and uniform), $|\mathcal{N}| = \{50, 100, 500, 1000, 5000\}$, and $K = \{2, 5, 10\}$ (from bottom to top on the horizontal axis). As expected, the CPU time to optimally solve the models grows as K grows, with some big jumps when moving from $K = 5$ to $K = 10$ (despite being less evident, this behavior is almost always respected also by the K-BACOP1 and K-BACOP2). Concerning the number of locations, instead, the CPU time is almost negligible for all the cases with $|\mathcal{N}| \leq 1000$. For these instances, only two spikes are visible (20.65s for K-BACOP2 on mono-polar instances with $|\mathcal{N}| = 500$ and $K = 10$, and 15.24s for K-DSM on uniform instances with $|\mathcal{N}| = 100$ and $K = 10$). Instead, for $|\mathcal{N}| = 5000$ the CPU times increase for all the models, with a particular effect on K-DSM, even if the average CPU time never exceeds 3 min. Note that such an increment affects the three topologies differently. For the multi-polar instances, the magnitude of the increment is much smaller than the one in the mono-polar ones. At the same time, the uniform case stays in between. Finally, note that, for K-BACOP1 and K-BACOP-2, the average CPU times for the instances with 5000 locations are always smaller than 12 s, thus making these models applicable on a huge scale. However, the 5-BACOP1 and 10-BACOP1 are often impossible to solve when $|\mathcal{N}|$ is small (this corresponds to the few missing yellow bars in the chart).

[5] Defining a particular policy to shut down the already located facilities would result in a too arbitrary choice, thus eliminating part of the generality of the results that we want to achieve.

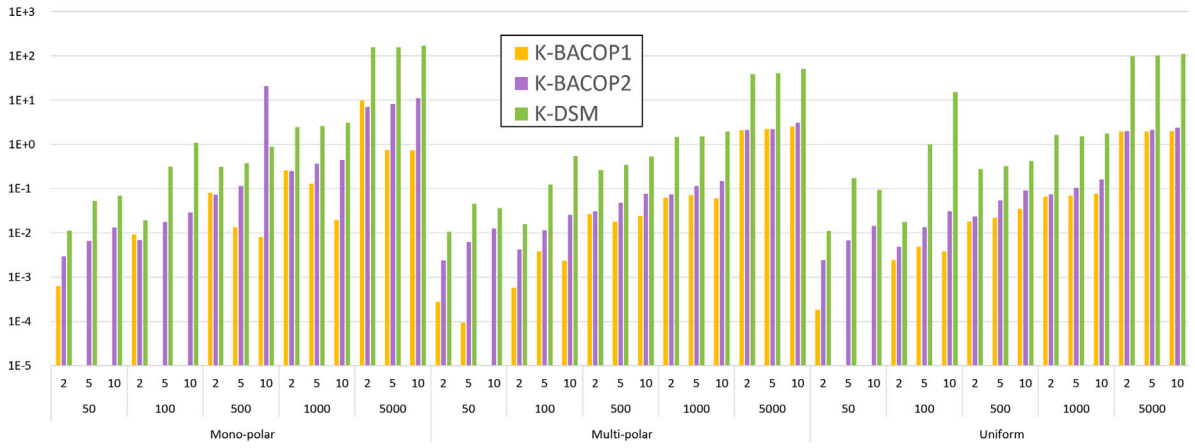

Fig. 1. CPU times.

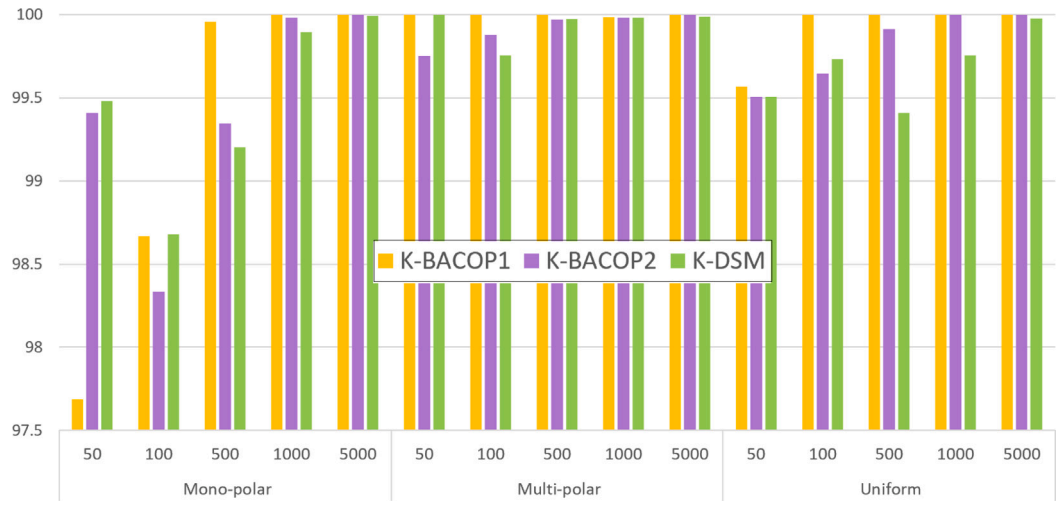

Fig. 2. Percentage of integer variables in the LP relaxation optimal solution.

To better understand the previous results, we further analyze the number of location variables (i.e., $y_i, i \in \mathcal{N}$) that are integers in the optimal solution of the continuous relaxation of the models. Fig. 2 shows the average percentage of such variables in the same experiments as above. Here, values are aggregated for each topology and different $|\mathcal{N}|$ (this time, the parameter K does not influence the analysis). First, note that the percentage of integer location variables seems to increase as $\mathcal{N}$ increases, and this is particularly evident in the mono-polar case. Second, all the reported averages are greater than 97.5%. Actually, if we exclude the smallest mono-polar instances ($\mathcal{N} \leq 100$), such averages never go below 99.2%. For multi-polar instances, all the models return a percentage of integer location variables in the LP relaxation always above the 99.7%. This justifies that almost all the models can be solved quickly, even if the underlying instances have an enormous number of locations or coverage levels to consider. This nice behavior is appreciable at the tactical level when hundreds of scenarios might need to be solved and compared.

7.2. KPI-based analysis

In the following, we report the results obtained from the KPI-based analysis in the case of static scenarios (Section 7.2.1) and of possible dynamic disruption of the already located facilities (Section 7.2.2). Since our instance generation works on parameters proportional to the instance dimension, for simplicity we focus the following analysis only on $|\mathcal{N}| = 100$. The tests involve a total of 960 instances, namely, 10 random instances for each combination of topology (mono-polar, multi-polar, and uniform), number of available facilities depending on $\gamma = \{0.2, \ldots, 0.9\}$, and covering radii depending on $(\mu_1, \mu_2) = \{(0.1, 0.25), (0.2, 0.3), (0.2, 0.5), (0.3, 0.5)\}$. For each KPI, only average values are reported and commented on. Since standard deviations are always negligible for all parameter combinations, we can consider the average as a trustworthy indicator.

7.2.1. KPIs results on static scenarios

Here, we discuss the KPIs presented in Section 6.2 in pure static scenarios. The entire experiment lasted about 9 h and a half, 96% of which was dedicated to solving the K-DSM (detailed CPU results can be found in Appendix A). Moreover, given the too-large number of infeasibilities returned by K-BACOP1 (see Appendix B), we will first compare K-BACOP2 with K-DSM only, and then perform a dedicated analysis including K-BACOP1 by focusing only on specific cases.

K-BACOP2 and K-DSM assessment through $avgC$ and $stdC$. We first consider the *weighted average coverage* ($avgC$) and the *standard deviation of the redundant coverage* ($stdC$), which are calculated as in (42) and (43), respectively. Fig. 3 reports the values of the two above KPIs for the optimal solution of the models averaged over all the generated instances given a specific tuple of input parameters $(\mu_1, \mu_2, \gamma, K)$. This tuple's value is reported on the horizontal axis from the bottom level to the top. Each chart relates to a specific distribution of the locations. The $avgC$ values (with the relative scale on the left) are colored in light violet and light green for K-BACOP2 and K-DSM, respectively, while

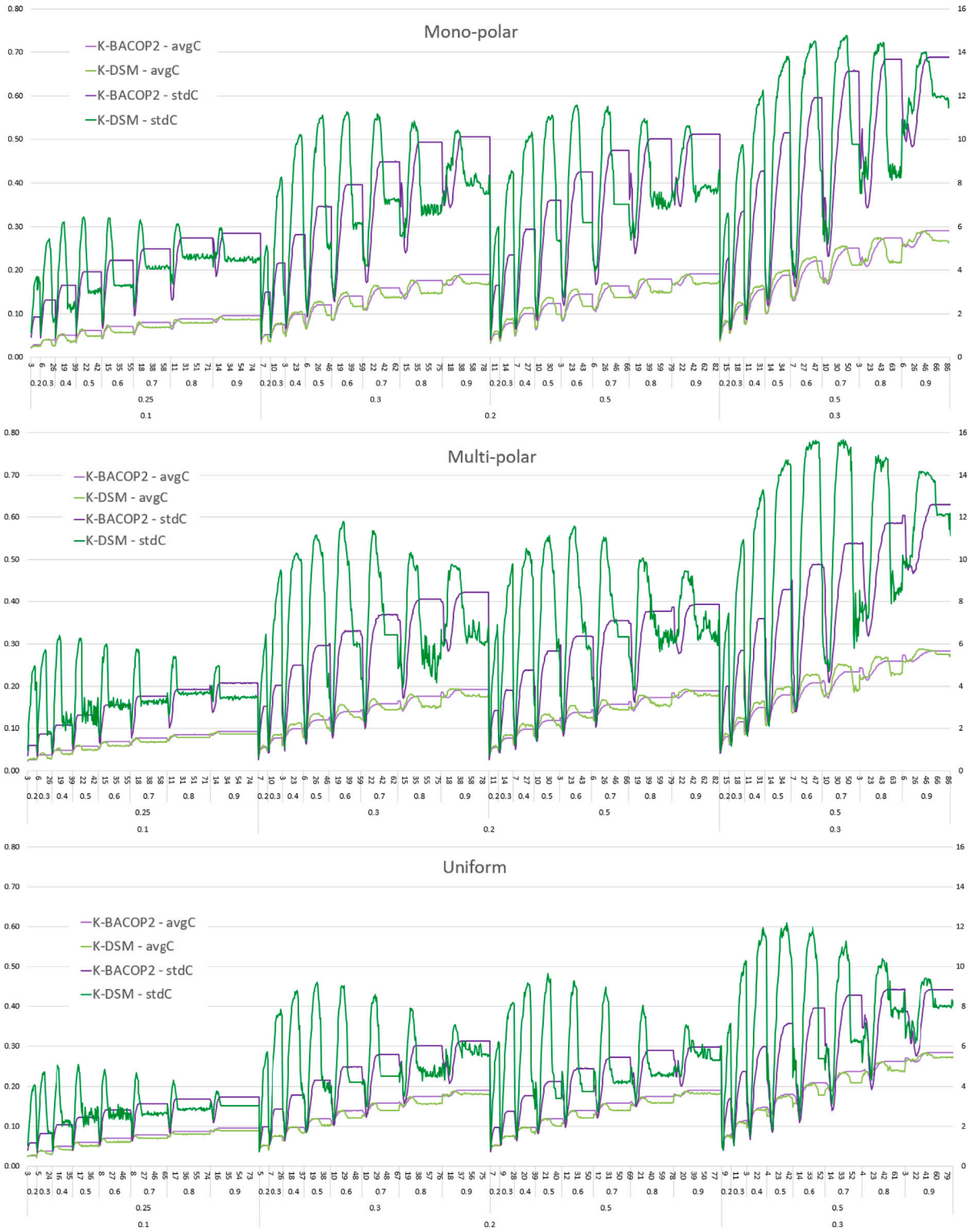

Fig. 3. *avgC* and *stdC* trends in K-BACOP2 and K-DSM solutions for mono-polar, multi-polar, and uniform instances.

stdC values (with the relative scale on the right) appear in the dark shade of the relative color for the two models.

The *avgC* KPI follows a relatively similar trend for each (μ_1, μ_2, γ) combination and each model, but changes in terms of the shapes' amplitude and of the minimum/maximum values obtained over the different Ks. The minimum and maximum KPIs values generally grow with the increase of available facilities, i.e., when γ increases, or with larger coverage radii. Simultaneously, their difference's amplitude seems more consistent for intermediate values of γ and the largest radii. This behavior is expected since the *avgC* indicator reflects the covering capability given by the coverage radii's width of the available facilities. Moreover, notice that, in general, lower values of γ yield less erratic trends for both the models when K increases. On the other hand, given a specific combination of (μ_1, μ_2, γ), the indicator over the increasing values of K is very interesting to analyze. First, note that K-DSM is unaffected by the increase of μ_2 for $\mu_1 = 0.2$. In mono-polar instances,

$avgC$ rapidly grows for both the models, with K-DSM achieving on average better results for smaller values of K. However, while K-BACOP2 steadily increases up to an asymptotic value and remains constant for the remaining values of K, K-DSM also rapidly decreases, after a peak, to a plateau value far worse than the corresponding for K-BACOP2. This behavior can also be found for the other instance distributions, even with some interesting peculiarities. In particular, for multi-polar instances, the difference between the two models in the initial phase is exacerbated, and the decreasing trend of K-DSM is less rapid. Moreover, the $avgC$ of both models initially decreases for several Ks before starting the above-described trend, with the highest variation for K-BACOP2. The better behavior of K-BACOP2 for minimal Ks is more evident when locating more available facilities. Concerning the uniform instances, instead, the initial peak of K-DSM rarely outperforms the relative value for K-BACOP2. This makes K-DSM particularly undesirable for uniform distributions in terms of average covering. Interestingly enough, for all the three instance distributions, K-DSM appears very competitive for the largest radii and small-medium values of γ (e.g., $\gamma \leq 0.5$), where the $avgC$ rarely decreases below the relative values of K-BACOP2.

The $stdC$ KPI has a behavior surprisingly similar to the $avgC$ trends, however, in this case, a higher value corresponds to a less equitable solution, i.e., a solution in which the worst-covered locations are covered very much less than the best-covered ones. We also remark that, differently from $avgC$, the models do not actually optimize equity measures in any way, so in this case, the $stdC$ values can be seen as a by-product of the coverage optimization. Notice that the $stdC$ KPI is particularly affected by the instance topology when γ tends to increase. In fact, for instances with a budget sufficient to locate a facility in almost all the locations, the $stdC$ can reach high values only because of the existence of locations placed at the very border of the considered area and far from the central, high-density region. As for $avgC$, both the minimum and the maximum values grow with the increase of the available facilities and the radii's width. This means that, if we are dealing with a service with a higher coverage radius, it is in general easier to cover more demand on average but also to provide a very inequitable coverage. The highest values of $stdC$ are achieved for the mono-polar instances and $(\mu_1, \mu_2, \gamma) = (0.3, 0.5, 0.7)$, while the uniform instances show lower values, even for the peaks. When looking at the $stdC$ behavior over the increase of K, almost always K-BACOP2 starts with lower values and smoothly grows to a plateau. K-DSM instead has a very rapid peak for the smaller values of K and then tends to decrease and fix to values smaller than the corresponding K-BACOP2 plateau. Actually, this last trend is more clear for the smallest radii, while for the larger ones, the K-DSM values are almost always higher than those of K-BACOP2 even with the increase of K. The peak behavior in K-DSM can be the result of its need to ensure first a total coverage of the demand within the smaller radius. Hence, such a requirement must be well-calibrated in order not to provide good coverage without considering the most unfortunate locations.

K-BACOP1 assessment through $avgC$ and $stdC$. Let us now focus on the K-BACOP1 performance, which can be compared only for a limited number of cases. Fig. 4 has the same layout used in Fig. 3 but including also the K-BACOP1 results ($avgC$ values in bright yellow and $stdC$ ones in darker). According to the feasibility results presented in Fig. B.10, here we only consider $\mu_1 = 0.3$, $\mu_2 = 0.5$, $\gamma \geq 0.3$, and small values of K ($K \leq 5$ for mono-polar and $K \leq 7$ for multi-polar and uniform instances). Note that, even if the following analysis relates to a very small part of our experiments, it makes much sense to be deepened since the large part of the real applications rarely consider very large values of K.

Concerning $avgC$, we can observe that K-BACOP1 almost always outperforms the other two models. In particular, K-BACOP1 performs very well for mono-polar and uniform instances and values of γ in between 0.3 and 0.7. The general increasing trend as γ increases, previously observed is maintained also in this specific set of instances and for the K-BACOP1 model. Again, middle values of γ yield the highest amplitude of values. In general, $avgC$ for K-BACOP1 decreases by increasing the value of K up to the level at which the problem becomes infeasible. However, the values start and stay above the K-BACOP2 ones in most cases. This means that K-BACOP1 is far from being a model to abandon since it can provide satisfactory results when the instance's feasibility is guaranteed (i.e., in general, for large coverage radii) and the desired level of coverage is limited. Note that this behavior is justified since K-BACOP1 has an objective function that, given a certain K, focuses on maximizing the coverage for that level, which in turn affects the coverage of lower levels. K-DSM has the same objective but is limited by the covering requirements on the larger radius. At the same time, K-BACOP2 waives most of the optimization effort at level K in favor of lower levels (the weighting factors in its objective function are such that a lower level is more important to cover more). If we observe the $stdC$ values, instead, no models totally outperform the others, and several cases must be discussed. For mono-polar and multi-polar instances, K-DSM is definitely the most equitable model, with relative gaps with respect to the others that grow as γ increases. While for multi-polar instances K-BACOP1 and K-BACOP2 perform very similarly, for mono-polar instances K-BACOP1 appears to be the less equitable model. The scenario changes if we consider uniform instances. Here, all the models tend to be more equitable and show quite similar performances. Actually, up to a value of $\gamma = 0.5$, K-DSM seems the worst model in terms of equity, with more discontinuous trends, while it becomes the best for a higher number of available facilities.

K-BACOP2 and K-DSM assessment against $C(k)$. The last part of this analysis is focused on the *weight of the kth coverage* $C(k)$, calculated as in (44). Fig. 5 reports the average value of $C(k)$ calculated in the optimal solution of K-BACOP2 and K-DSM over all the generated instances given a specific combination of parameters γ and K (horizontal axis) and a specific value of k (different shades of the same color). Each chart relates to a specific distribution of the locations. Note that instances are not distinguished by radii anymore since in the previous tests we have seen that such trends are similar and the only difference is in terms of the value of convergence. Moreover, even if we have calculated $C(k)$ for any $k = 1, \ldots, |\mathcal{N}|$, we show in the figure only a sample of 5 values (namely, $k = \{1, 5, 10, 15, 20\}$). This sample is representative since, for k in between 21 and 47 (the maximum topological limit $\bar{k}$ for the generated instances), the $C(k)$ value becomes negligible and does not add anything to the analysis. First, notice that the KPI values and behaviors are not significantly affected by the topology of the instances, even if, for the mono-polar ones, the gap between $k = 1$ and $k = 5$ is larger than the gap observed in the other two cases. In a mono-polar instance, in fact, having most of the demand concentrated around a single zone, it is more challenging to guarantee very high coverage, even considering small values of k. Similarly, there is a more significant gap between the values for $k = 5$ and $k = 10$ in multi-polar instances, where the demand is still concentrated but around different poles. Moreover, as for the previously presented KPIs, the minimum and maximum values as well (as the difference between them) grow as the number budget on facilities increases, with marked changes for middle values of γ and higher values of k. However, the most interesting aspect to analyze is again related to the two models' behavior with respect to the increase of K. Here, we can observe that the trends for the different Ks are somehow similar to those observed for the $avgC$ indicator. K-BACOP2 shows a very smooth trend, whereas K-DSM a more erratic one. In general, for both models, the best value is obtained for a K equal to k. Nevertheless, while K-BACOP2 tends to reach a stable value, K-DSM rapidly decreases in most cases and reaches minima far below the relative values of K-BACOP2. Several times, as already seen for the $avgC$ indicator, K-DSM achieves rapidly higher peaks, but the

Fig. 4. *avgC* and *stdC* trends in the three models solutions for mono-polar, multi-polar, and uniform instances.

performances also worsen rapidly after the peak. In very rare cases, as for multi-polar instances, $\gamma = 0.8$, and $k = 10$, K-DSM outperforms K-BACOP2 for higher values of K. Finally, an important thing to notice is that K-DSM cannot guarantee total coverage in most cases even considering $k = 1$ (which relates to the fraction of demand covered at least once within r_1), with minima around 90% for small values of γ. This is because K-DSM must ensure coverage for the larger radius r_2 and cannot only optimize the coverage redundancy within r_1.

7.2.2. KPIs results for dynamic scenarios with disruption

We now assess the three models' performances mentioned above of K-covering models by explicitly simulating disruption events. The general simulation setting is the one described in Section 6.3, where, for a given K, we consider only values of γ such that $p = |\mathcal{N}| \cdot \gamma \geq p_{min}$ to guarantee always a feasible solution. The procedure is repeated 100 times to have average KPIs that are statistically meaningful. Particular attention will be given to the parameter ϵ, representing the *degree of*

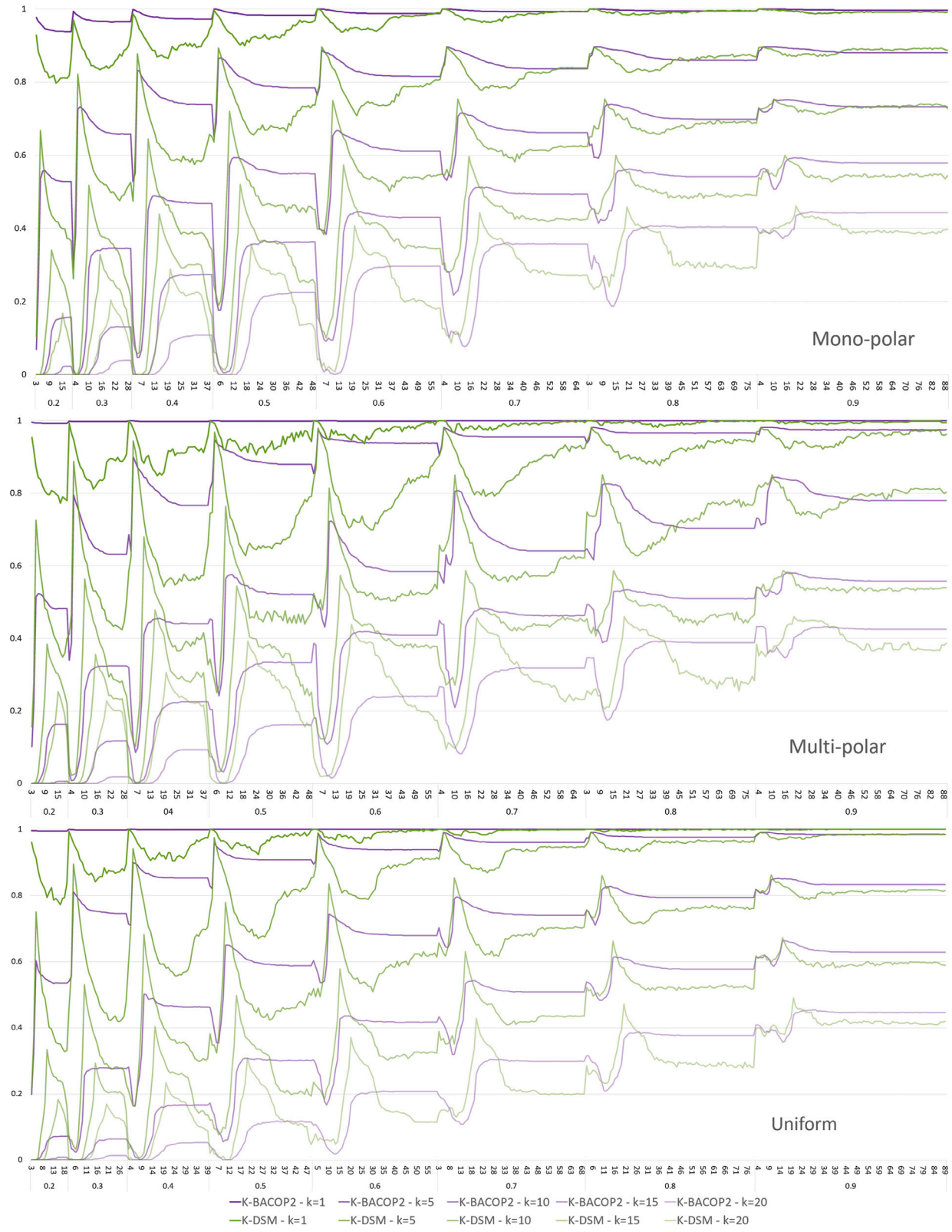

Fig. 5. $C(k)$ trends in K-BACOP2 and K-DSM solutions for mono-polar, multi-polar, and uniform instances.

disruption. As an indicator for the analysis, we consider again the *k-level weighted coverage* $C(k)$ calculated as in (44), because of its easy interpretation. It represents the percentage of demand covered at least k times. Hence, since the demand is generated such that $\sum_{i \in \mathcal{N}} h_i = 1$, $C(k)$ will be equal to 1 when all locations are covered at least k times. Moreover, by considering different values of k, it is possible to investigate how the models behave concerning different coverage levels. Fig. 6 shows the average value of $C(k)$ calculated on the optimal solution of K-BACOP1, K-BACOP2, and K-DSM over all the generated instances given a specific value of parameter ε (horizontal axis) and a particular value of k (different shades of the same color). Each chart relates to a specific distribution of the locations. Again, even if we have

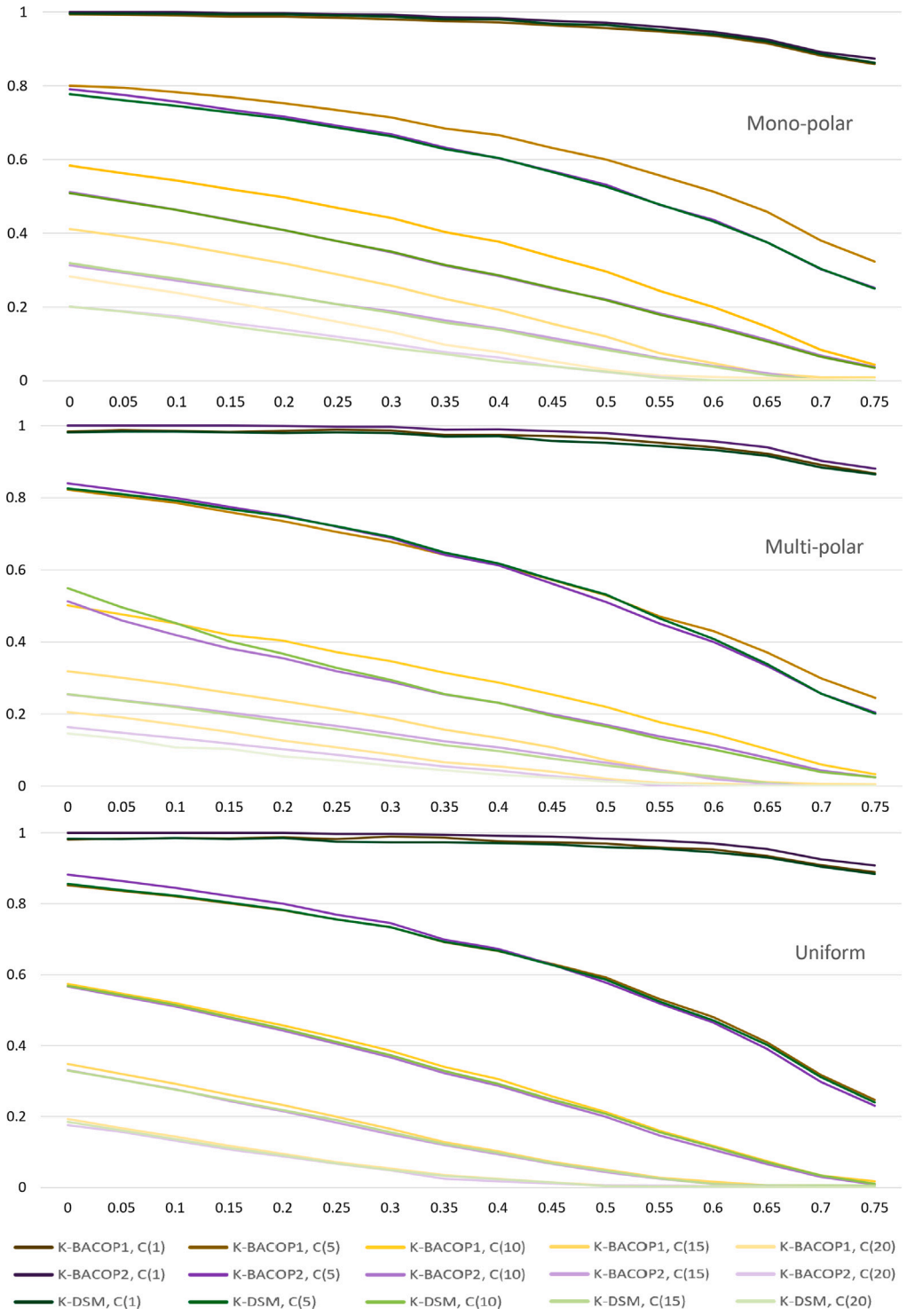

Fig. 6. Average $C(k)$ variation of K-BACOP1, K-BACOP2 and K-DSM solutions for mono-polar, multi-polar, and uniform instances against different degrees of disruption ε.

calculated $C(k)$ for any $k = 1, \ldots, |\mathcal{N}|$, we show in the figure only a sample of 5 values (namely, $k = \{1, 5, 10, 15, 20\}$). Note that, since we are interested in the model properties, on the horizontal axis, it is reported only the value of ε because each value is obtained as the average over all the other parameters (γ, μ_1, μ_2, K).

The first thing we can notice is that, as expected, all the curves have a decreasing behavior. Unexpectedly, instead, the curves for $C(1)$ decrease very slightly, and, for a disruption of 75%, the KPI settles at values around or higher than 0.9. This is good news since all the solutions cover the vast majority of the locations at least once, even if a high value of disruption appears. This property is of paramount importance in healthcare applications. The rate of decay of $C(k)$ for any $k > 1$ is greater than the one for $k = 1$. This means that the marginal value of adding a facility increases as the level of coverage increases. In other words, the higher the coverage level considered, the more adding a new facility is important. This is also the reason for the different curvatures for different values of k. In fact, as the reader can notice, the curves of the $C(1)$ and $C(5)$ are concave, while the curves of $C(10)$, $C(15)$ and $C(20)$ tend to a convex shape.

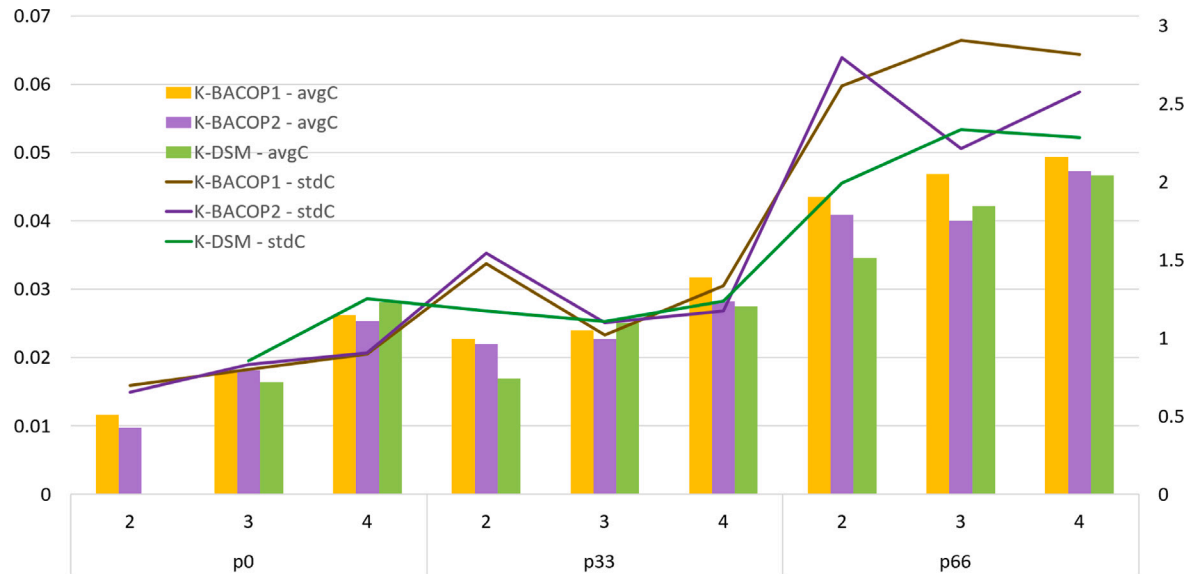

Fig. 7. Case study results of $avgC$ and $stdC$ for the three models. Bars correspond to $avgC$ values (with relative scale on the left), while lines correspond to $stdC$ values (with relative scale on the right).

Comparing the different models' performance, we notice that the trends for $k = 1$ are almost the same for all the models. There are just some slight differences in the multi-polar and uniform instances, in which K-BACOP2 is slightly better than the other two models. Nevertheless, these differences are not statistically significant since the standard deviation of the considered values is such that the confidence intervals overlap for reasonable confidence. Instead, the situation is very different for the other values of k. In general, K-BACOP1 performs better than the other two models especially for small and medium degrees of disruption, confirming its importance despite the already exploited intrinsic infeasibility issues. This superiority, clear in the mono-polar instances, becomes less evident in the multi-polar and uniform instances. In particular, in this last case, all three models perform very closely. To understand this result, it is essential to remember that no one of the considered models pursues the optimization of the *k-level weighted coverage* or explicitly considers disruption events. Thus, the performance difference is related to the by-product value of the robustness of the models' solutions. Therefore, it is reasonable that the models perform similarly in the uniform instances, where the locations are topologically equivalent. Instead, in the multi-polar instances, the locations are not topologically identical, and this difference generates the variations that we can observe from the graph. Nevertheless, since locations are organized in clusters, most models locate facilities in the clusters' centers. Thus the robustness of the solution is nearly the same for all the models. Finally, in the mono-polar instances, the locations' topological characteristics are different (e.g., the locations in the center of the graph are more attractive because they can cover several other locations, while the locations on the border are less attractive because they can cover fewer locations). Moreover, the number of locations with similar topological importance is significant enough to let the models choose very different solutions. This leads to the very different performances that the reader can observe in the chart.

Finally, we want to discuss why K-BACOP1 has such a good performance. The reason is the same as the one reported in Section 7.2.1. K-BACOP1 has an objective function that focuses on maximizing only the Kth coverage of the demand (and not all the levels as K-BACOP2). Furthermore, since it does not have to fulfill other covering requirements (as it happens for K-DSM outer radius), it has total freedom to concentrate the location effort on standard covering. These two characteristics allow K-BACOP1 to find more robust solutions since disruption events can hardly eliminate the entire maximum-level coverage given by such a model to the demand locations.

8. A case study on ambulances location

In this section, we conduct a similar analysis for a real case study concerning the ambulance service in the Fez-Meknes region of Morocco, which has more than 1.7 million inhabitants and includes the second-largest city in Morocco. Being a populated region with a big city in the center, its topology resembles a mono-polar instance. The road network of the region provides a unique highway that goes from East to West and five perpendicular high-speed roads. We build upon the dataset proposed in Frichi et al. [74] that contains the set of all the municipalities of the region (each one identified by its coordinates) and the corresponding demand in terms of the total number of calls received and processed by the *Civil Protection Alert Processing Center*. We compute the demand rate of each city as the normalized number of calls and we derive the distance matrix by means of the *open street map* APIs. The covering sets are constructed by assuming $r_1 = 15$ min, $r_2 = 10$ min, and an average ambulance speed of 100 km/h.

Our analysis consists in the calculation of the proposed KPIs on different solutions for $K = 2, 3$, and 4 and for three different values of p, namely, $p0 = p_{min}$, $p33 = p_{min} + \frac{1}{3}(|\mathcal{N}| - p_{min})$, and $p66 = p_{min} + \frac{2}{3}(|\mathcal{N}| - p_{min})$. These values represent reasonable levels of covering and budget investment. On one side, $p0$ represents the minimum investment that enables the covering of all the cities $K - 1$ times, allowing us to obtain a feasible solution for almost all the cases and models. On the other side, $|\mathcal{N}|$ is the greatest possible investment, i.e., an ambulance in each location, thus $p33$ and $p66$ represent two intermediate interventions. The results are reported in Figs. 7 and 8. As before, K-BACOP1 results are colored in yellow, K-BACOP2 results in purple, and K-DSM results in green. Data are grouped per values of (p, K).

In Fig. 7, we can see that 2-DSM is infeasible for $p0$, i.e., with the considered number of facilities it is not possible to satisfy constraints (31). Since augmenting K, also $p0$ increases, The model becomes feasible in the other cases since K slightly increases while p increases by a large amount. Analyzing $avgC$, we can notice that it increases as K and p increase. Interestingly, using $p0$ facilities with $K = 4$ leads to results comparable to the one achieved using $p33$ with $K = 2$ or $K = 3$. These results are even more impressive if we consider that $p0 = 49$ for $K = 4$, while $p33 = 61$ for $K = 2$ and $p33 = 75$ for $K = 3$. Therefore, with a smaller number of facilities, we can achieve a better level of $avgC$. The evolution of the $stdC$ tends to decrease as K increases for $p33$ and $p66$. This is the same behavior that can be observed in the previous section. Therefore, from the equity point of view, a lower

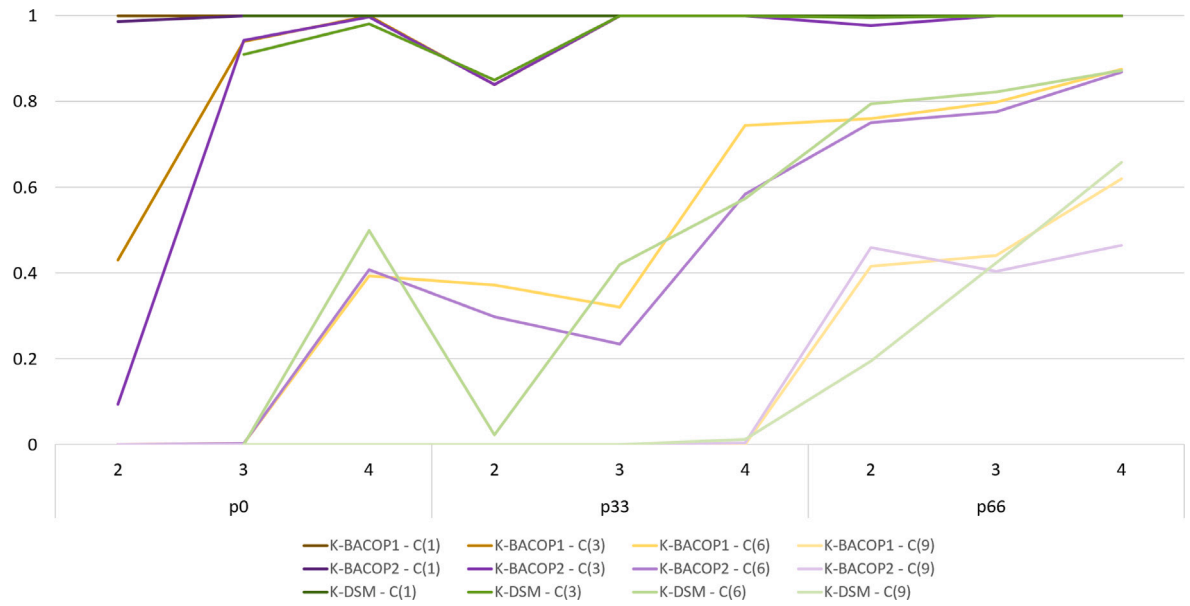

Fig. 8. Case study results of $C(k)$ for the three models. We reported $C(k)$ values for $k = \{1, 3, 6, 9\}$. For each model, the higher the value of k, the lighter the relative color.

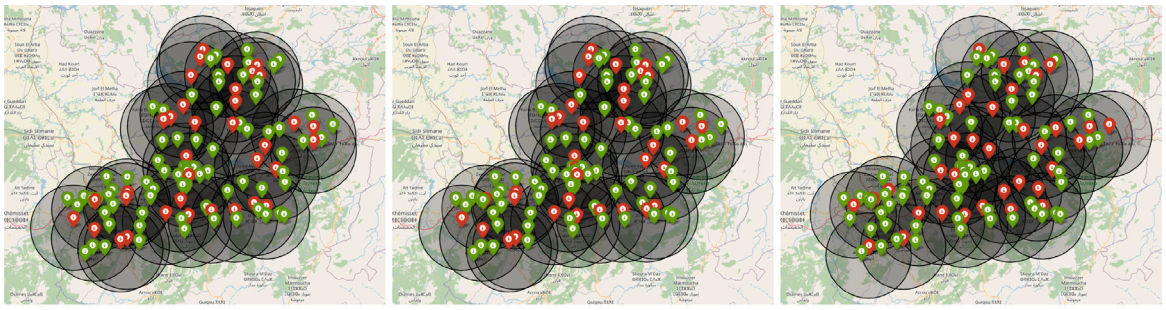

(a) (b) (c)

Fig. 9. Different solutions (a) K-BACOP1, (b) K-BACOP2, (c) K-DSM for $K = 3$.

amount of facilities and higher values of K must be preferred. The same conclusion obtained for $avgC$ holds also for the $stdC$, where the best model seems to be the ones with $p0 = 49, K = 4$. From these observations, we can get some first managerial insight. In fact, there seems to be no point in allocating a quantity of ambulance $p = p33$ since better results can be achieved by installing fewer ambulances. Of course, if the available budget is enough the optimal solution would be to install $p = p66$ ambulances to increase the values of $avgC$. Nevertheless, when installing $p = p66$ ambulances, $stdC$ increases by many times, therefore it would be nice to lower this parameter by adding new possible stations for the ambulances. Finally, while for $p = p0$ it is better to consider $K = 4$ and the best model seems to be the K-DSM, for $p = p66$ it is better to consider $K = 3$ which presents the better trade-off between $avgC$ and $stdC$, and the model that behaves better is the K-BACOP1. Finally, by observing the $C(k)$ trends in Fig. 8, similar conclusions can be drawn. Almost all the models cover all the facilities at least once. Therefore with all the models, a good covering is guaranteed, even with a minimal investment equal to $p = p0$. In particular, the results for the K-DSM with $p = p0$ are comparable with the ones obtained with $p = p33$. This enforces the claim that a small investment with just p_{min} facilities, located according to the K-DSM can have really good performances.

To better grasp the characteristics of the solutions of the different models, we plot on the geographical map three of them with $p = p33$ and $K = 3$ in Fig. 9. Among all the municipalities in green, the red beacons represent the located facilities and a circle corresponds to the area covered. Note that such circles are just approximations of the real covering sets since, due to the asymmetry of the travel distances, the covered area has a more complex shape. As the reader can notice, the solutions of 3-BACOP1 and 3-BACOP2 are really close to each other, only differing for a few locations. This behavior is reasonable since, for these small values of K, 3-BACOP2 cannot dissipate too much coverage in favor of lower levels and thus performs very similarly to 3-BACOP1. Instead, the solution of the 3-DSM differs significantly from the other two since it better covers the central areas. This is due to constraints (31) which require covering a given percentage of demand with a smaller radius and this is accomplished by the most central area, in which the greater city of the region is placed.

9. Conclusions

This paper has studied covering facility location problems, focusing on coverage redundancy for the underlying service. This aspect is particularly critical in many applications (e.g., in healthcare and emergency services), where it is essential to provide robust location solutions to avoid disruption or congestion of the already located facilities. We introduced and studied three families of parametric models (namely, K-BACOP1, K-BACOP2, and K-DSM) that generalize three classical double-covering models from the literature. The generalizations can address any Kth level of coverage greater than two and provide insightful strategic location tools. The models are compared both theoretically and empirically. In particular, apart from their efficiency, we assessed

Table A.2
Comparison of the models in terms of CPU time (s).

γ	Mono-polar			Multi-polar			Uniform		
	K-BACOP1	K-BACOP2	K-DSM	K-BACOP1	K-BACOP2	K-DSM	K-BACOP1	K-BACOP2	K-DSM
0.2	0.5	13.0	1255.2	1.1	10.1	653.0	2.2	11.8	4490.1
0.3	0.9	27.8	1339.1	1.7	24.0	713.8	2.3	26.5	7117.8
0.4	1.1	42.0	796.7	2.0	39.0	379.8	2.3	41.8	8334.2
0.5	1.3	57.6	407.2	2.1	54.0	187.4	2.3	59.3	5260.1
0.6	1.6	73.5	166.2	2.2	69.9	92.9	2.5	77.6	1861.4
0.7	1.9	89.1	89.1	2.4	86.6	58.0	2.7	92.3	406.6
0.8	2.2	104.7	60.2	2.5	103.6	51.1	2.7	105.7	105.3
0.9	2.6	119.1	58.2	2.7	118.4	51.5	2.7	120.5	54.6
Sum:	12.1	527.0	4171.8	16.7	505.6	2187.6	19.6	535.7	27 630.1
Avg:	1.5	65.9	521.5	2.1	63.2	273.4	2.4	67.0	3453.8
Stdev:	0.7	37.4	539.3	0.5	38.4	276.3	0.2	38.7	3298.7

the solutions' quality returned by the models concerning redundancy aspects through a comparative simulation–optimization framework and tailored KPIs.

Our experiments, conducted over many representative instances with different topological characteristics and simulating disruption scenarios for the located facilities, allowed us to derive interesting managerial insights. For example, CPU times are minimal even against huge instances (5000 locations and 10 coverage levels to consider). Moreover, we noticed that K-DSM outperforms K-BACOP2 for small values of K both in terms of average coverage and equity, but its performances decay rapidly, making K-BACOP2 a more robust choice when considering higher levels of coverage. K-BACOP1, instead, clearly suffers from the feasibility point of view. However, for sufficiently large radii and small desired levels of coverage, it performs very well in terms of average coverage (both with and without disruption simulation) because it is focused on optimizing the highest level of coverage considered. Nevertheless, its equity performance strongly depends on the instance topology. The generality of the results obtained from this analysis has been further validated over a real case study concerning the ambulance service in Morocco.

Some future research lines can be highlighted. First, the proposed deterministic models can be evaluated in a more sophisticated stochastic setting, where some problem uncertainties (e.g., the demand) are explicitly considered. Concerning the well-known multi-stage Stochastic Programming paradigm, the different coverage levels may be addressed at different information stages. Since these models are challenging to solve concerning their deterministic counterparts, tailored solutions or approximation methods must be derived. Second, the redundancy of the coverage could be studied also for a time-dependent setting in which covering sets vary over time [75]. Third, a similar analysis could be performed on all those services with relevant social implications such as the location of electric vehicle recharging stations [76,77] or urban stops for public transportation [78]. Finally, it would be interesting to investigate how the topological properties, e.g. $\bar{k}$ or p_{min} (see Sections 6.2 and 6.3, respectively), interact with the solutions of the optimization models proposed.

CRediT authorship contribution statement

Edoardo Fadda: Conceptualization, Formal analysis, Investigation, Methodology, Software, Validation, Writing – original draft. **Daniele Manerba:** Conceptualization, Formal analysis, Methodology, Project administration, Visualization, Writing – original draft, Writing – review & editing. **Roberto Tadei:** Conceptualization, Supervision, Writing – review & editing.

Data availability

Data will be made available on request.

Acknowledgments

The second author has been supported by "ULTRAOPTYMAL - Urban Logistics and sustainable TRAnsportation: OPtimization under uncertainTY and MAchine Learning", a PRIN2020 project funded by the Italian University and Research Ministry (n. 20207C8T9M, https://ultraoptymal.unibg.it). All the authors are grateful to two anonymous reviewers who contributed, through their constructive comments, to the quality of the paper.

Appendix A. Detailed CPU results for $|\mathcal{N}^*|$=100 instances

Table A.2 reports, for each distribution type (mono-polar, multi-polar, and uniform) and each family of models (K-BACOP1, K-BACOP2, and K-DSM), the average CPU time needed by the MIP solver to optimally solve all the instances generated. It is worth noting that we consider only instances that are feasible for all the models. Instances are grouped by the value of γ, which affects the number p of facilities to locate. Note that, in each group, the number of instances is different since the increase of K is bounded by p. The higher the value of γ, the higher the number of considered instances.

Some clear trends can be highlighted. K-BACOP1 problems are straightforward to solve, with an accumulated CPU time per γ of 2 s on average and never exceeding 3 s. For this model, the mono-polar instances seem easier to solve, while the uniform is the hardest. In general, considering that the number of problems to solve linearly increases with the increase of γ, we can say that K-BACOP1 is not significantly affected by the value of γ in terms of CPU time. Concerning K-BACOP2 problems, they need, in general, a CPU time that is 1 or 2 orders of magnitude greater than those of K-BACOP1. Interesting enough, the accumulated CPU time increases with γ with a linear trend. This means that the difficulty of solving K-BACOP2 problems decreases by increasing the number of facilities to locate. Unlike the other two families of models, K-BACOP2 seems not significantly affected by the locations' distribution, with only slightly higher CPU times for the uniform instances and somewhat lower for the multi-polar ones. K-DSM problems result in the most difficult to solve. The total CPU time is on average about 8 times, 4 times, and 50 times greater than that of K-BACOP2 for mono-polar, multi-polar, and uniform instances, respectively. In particular, K-DSM seems very difficult to solve for uniform instances. However, it is interesting to notice K-DSM concerning γ, which differs from K-BACOP1 and K-BACOP2. In particular, with small values of γ, the CPU time is already very high, rapidly increases to find a peak, and decreases consistently for higher values of γ. The peak is at $\gamma = 0.3$ for mono-polar and multi-polar instances, while it is at $\gamma = 0.4$ for the uniform ones. Interesting enough, for very high values of γ (see, e.g., $\gamma \geq 0.8$ for the uniform instances and $\gamma \geq 0.7$ for mono-polar and multi-polar ones), the resolution of K-DSM seems to be similar or even more straightforward than that of K-BACOP2.

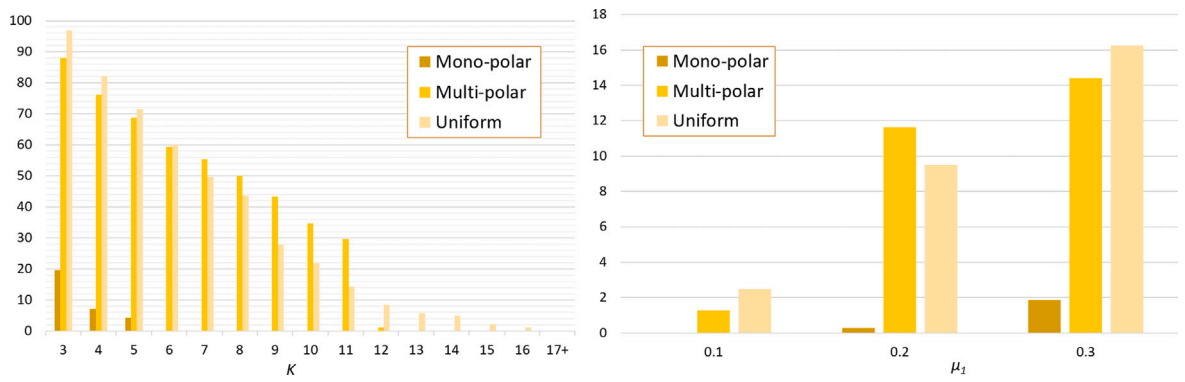

Fig. B.10. Percentage of feasible instances for K-BACOP1.

Appendix B. Detailed results on K-BACOP1 infeasibility for $|\mathcal{N}|=100$ instances

While K-BACOP2 cannot lead to infeasible solutions, this is not true for K-BACOP1, for which a feasible instance requires to guarantee the $(K-1)$-covering of all the demand centers (see Section 4.1), and for K-DSM, for which a certain percentage of the demand $\alpha^{(k)}$ must be ensured for each level K of coverage. Our generation of $\alpha^{(k)}$ (see Section 6.1) has been done so that it is highly improbable to fall into infeasible cases for K-DSM. Indeed, we never obtained infeasible solutions from K-DSM in our experiments. Instead, K-BACOP1 returned a significant amount of infeasible solutions, making necessary a tailored analysis. Fig. B.10 reports, for the different distribution types, the percentage of feasible solutions obtained by K-BACOP1 concerning the total number of considered instances, grouped by K (left chart) and by covering radius μ_1 (right chart). The percentage of feasible solutions rapidly decreases with the increase of the considered level of coverage K. However, there are clear differences among the three distribution types. In mono-polar instances, only the 20% of instances are feasible for $K=3$, and no feasible solutions can be found for $K \geq 6$. This is reasonable since the demand is mainly concentrated around one area while other locations could be very far from there. When the demand is more distributed, as, in multi-polar and uniform instances, feasible solutions appear for a more considerable value of K, even if they vanish for values greater than 12 and 16, respectively. In total, only about the 6% of the tested instances are feasible for K-BACOP1. It can be seen from the chart on the right, most of them relate to the medium and the greatest radii (around 10% and 15%, respectively). This behavior depends on the particular way in which instances have been generated. However, K-BACOP1 can be useful in realistic settings only for small desired levels of coverage K, medium–large coverage radii, and good dispersion of the locations.

Finally, note that the significant amount of infeasible problems is a clear cause for the negligible CPU times reported in Table A.2 concerning K-BACOP1. In general, MIP solvers can detect infeasibility very fast.

References

[1] Laporte G, Nickel S, da Gama FS. Location science. Springer International Publishing; 2015.

[2] Giusti R, Manerba D, Tadei R. Multiperiod transshipment location–allocation problem with flow synchronization under stochastic handling operations. Networks 2021;78(1):88–104.

[3] Kain R, Manerba D, Tadei R. The index selection problem with configurations and memory limitation: A scatter search approach. Comput Oper Res 2021;133:105385.

[4] Burkey M, Bhadury J, Eiselt H. A location-based comparison of health care services in four U.S. states with efficiency and equity. Socio-Econ Plan Sci 2012;46(2):157–63.

[5] Barbati M, Piccolo C. Equality measures properties for location problems. Optim Lett 2016;10:903–20.

[6] Ibarra-Rojas O, Ozuna L, López-Piñón D. The maximal covering location problem with accessibility indicators. Socio-Econ Plan Sci 2020;71:100758.

[7] Vicencio-Medina SJ, Rios-Solis YA, Ibarra-Rojas OJ, Cid-Garcia NM, Rios-Solis L. The maximal covering location problem with accessibility indicators and mobile units. Socio-Econ Plan Sci 2023;87:101597.

[8] García S, Marín A. Covering location problems. In: Laporte G, Nickel S, Saldanha da Gama F, editors. Location science. Cham: Springer International Publishing; 2019, p. 99–119.

[9] Zhang B, Peng J, Li S. Covering location problem of emergency service facilities in an uncertain environment. Appl Math Model 2017;51:429–47.

[10] Bruno G, Cavola M, Diglio A, Piccolo C. Improving spatial accessibility to regional health systems through facility capacity management. Socio-Econ Plan Sci 2020;71:100881.

[11] Wang W, Wu S, Wang S, Zhen L, Qu X. Emergency facility location problems in logistics: Status and perspectives. Transp Res Part E: Logist Transp Rev 2021;154:102465.

[12] Brotcorne L, Laporte G, Semet F. Ambulance location and relocation models. European J Oper Res 2003;147:451–63.

[13] Hogan K, ReVelle C. Concepts and applications of backup coverage. Manage Sci 1986;32:1434–44.

[14] Gendreau M, Laporte G, Semet F. Solving an ambulance location model by tabu search. Locat Sci 1997;5:75–88.

[15] Klibi W, Martel A, Guitouni A. The impact of operations anticipations on the quality of stochastic location-allocation models. Omega 2016;62:19–33.

[16] Fadda E, Manerba D, Cabodi G, Camurati PE, Tadei R. Comparative analysis of models and performance indicators for optimal service facility location. Transp Res Part E: Logist Transp Rev 2021;145:102174.

[17] Butt SE, Cavalier TM. Facility location in the presence of congested regions with the rectilinear distance metric. Socio-Econ Plan Sci 1997;31(2):103–13.

[18] Jain K, Vazirani VV. An approximation algorithm for the fault tolerant metric facility location problem. Algorithmica 2003;38(3):433–9.

[19] Swamy C, Shmoys DB. Fault-tolerant facility location. ACM Trans Algorithms 2008;4(4).

[20] Vasilyev I, Ushakov AV, Maltugueva N, Sforza A. An effective heuristic for large-scale fault-tolerant k-median problem. Soft Comput 2018;23(9):2959–67.

[21] Baumann P. FT-KMEANS: A fast algorithm for fault-tolerant facility location. In: 2022 IEEE international conference on industrial engineering and engineering management (IEEM). IEEE; 2022.

[22] Church RL, ReVelle CS. The maximal covering location problem. Pap Reg Sci Assoc 1974;32:101–18.

[23] Daskin MS, Stern EH. A hierarchical objective set covering model for emergency medical service vehicle deployment. Transp Sci 1981;15:137–52.

[24] Doerner KF, Gutjahr WJ, Hartl RF, Karall M, Reimann M. Heuristic solution of an extended double-coverage ambulance location problem for Austria. CEJOR Cent Eur J Oper Res 2005;13:325–40.

[25] Doerner K, Hartl R. Health care logistics, emergency preparedness, and disaster relief: New challenges for routing problems with a focus on the Austrian situation. In: Golden B, Raghavan S, Wasil E, editors. The vehicle routing problem: latest advances and new challenges. operations research/computer science interfaces. 43, Springer, Boston, MA; 2008.

[26] Current J, O'Kelly M. Locating emergency warning sirens. Decis Sci 1992;23:221–34.

[27] Moore GC, ReVelle C. The hierarchical service location problem. Manage Sci 1982;28:775–80.

[28] Mitropoulos P, Mitropoulos I, Giannikos I, Sissouras A. A biobjective model for the locational planning of hospitals and health centers. Health Care Manag Sci 2006;9:171–9.

[29] Marianov V. Location models for emergency service applications. INFORMS Tutor Oper Res 2017.

[30] Ahmadi-Javid A, Seyedi P, Syam SS. A survey of healthcare facility location. Comput Oper Res 2017;79:223–63.
[31] Armacost RL. A 0-1 nonlinear programming model for coast guard fisheries law enforcement aircraft patrols. European J Oper Res 1992;56:134–45.
[32] Simpson NC, Hancock PG. The incident commander's problem: resource allocation in the context of emergency response. Int J Serv Sci 2009;2:102–24.
[33] Green LV, Kolesar PJ. Improving emergency responsiveness with management science. Manage Sci 2004;50.
[34] Karasakal O, Karasakal EK. A maximal covering location model in the presence of partial coverage. Comput Oper Res 2004;31:1515–26.
[35] Berman O, Krass D, Drezner Z. The gradual covering decay location problem on a network. European J Oper Res 2003;151:474–80.
[36] Berman O, Wang J. The minmax regret gradual covering location problem on a network with incomplete information of demand weights. European J Oper Res 2011;208:233–8.
[37] Drezner Z, Wesolowsky GO, Drezner T. The gradual covering problem. Naval Res Logist 2004;51:841–55.
[38] Eiselt H, Marianov V. Gradual location set covering with service quality. Socio-Econ Plan Sci 2009;43:121–30.
[39] Cordeau JF, Furini F, Ljubic I. Benders decomposition for very large scale partial set covering and maximal covering location problems. European J Oper Res 2019;275:882–96.
[40] Chanta S, Sangsawang O. Solving maximal covering location problem by using dynamic programming. In: IE network conference. 2012, p. 2364–7.
[41] Galvão RD, ReVelle C. A Lagrangean heuristic for the maximal covering location problem. European J Oper Res 1996;88:114–23.
[42] Gendreau M, Laporte G, Semet F. The maximal expected coverage relocation problem for emergency vehicles. J Oper Res Soc 2006;57:22–8.
[43] Gendreau M, Laporte G, Semet F. A dynamic model and parallel tabu search heuristic for real-time ambulance relocation. Parallel Comput 2001;27:1641–53.
[44] Li X, Zhao Z, Zhu X, Wyatt T. Covering models and optimization techniques for emergency response facility location and planning: A review. Math Methods Oper Res 2011;74:281–310.
[45] Sung I, Lee T. Scenario-based approach for the ambulance location problem with stochastic call arrivals under a dispatching policy. Flex Serv Manuf J 2018;30:153–70.
[46] MirHassani S, Khaleghi A, Hooshmand F. Two-stage stochastic programming model to locate capacitated EV-charging stations in urban areas under demand uncertainty. EURO J Transp Logist 2020;9:100025.
[47] ReVelle C, Hogan K. The maximum availability location problem. Transp Sci 1989;23:192–200.
[48] Daskin MS. A maximum expected covering location model: Formulation, properties and heuristic solution. Transp Sci 1983;17:1–113.
[49] Sorensen P, Church R. Integrating expected coverage and local reliability for emergency medical services location problems. Socio-Econ Plan Sci 2010;44:8–18.
[50] Rajagopalan HK, Saydam C, Xiao J. A multiperiod set covering location model for dynamic redeployment of ambulances. Comput Oper Res 2008;35:814–26.
[51] Chelst K, Jarvis JP. Estimating the probability distribution of travel times for urban emergency service systems. Oper Res 1979;27:199–204.
[52] Drezner T, Drezner Z, Goldstein Z. A stochastic gradual cover location problem. Naval Res Logist 2010;57:367–72.
[53] Drakulic D, Takaci A, Maric M. New model of maximal covering location problem with fuzzy conditions. Comput Inform 2016;35:635–52.
[54] nez JAS, Carlo HJ. Reliable capacitated facility location problem with service levels. EURO J Transp Logist 2018;7:315–41.
[55] Snyder LV. Facility location under uncertainty: A review. IIE Trans 2006;18:547–64.
[56] Snyder LV, Daskin MS. Reliability models for facility location: The expected failure cost case. Transp Sci 2005;39:400–16.
[57] Cui T, Ouyang Y, Shen ZJM. Reliable facility location design under the risk of disruptions. Oper Res 2010;58:998–1011.
[58] Shen ZJM, Zhan RL, Zhang J. The reliable facility location problem: Formulations, heuristics, and approximation algorithms. INFORMS J Comput 2011;23:470–82.
[59] Lu M, Ran L, Shen ZJM. Reliable facility location design under uncertain correlated disruptions. Manuf Serv Oper Manag 2015;17:445–55.
[60] Pouraliakbari-Mamaghani M, Saif A, Kamal N. Reliable design of a congested disaster relief network: A two-stage stochastic-robust optimization approach. Socio-Econ Plan Sci 2023;86:101498.
[61] Gourtani A, Nguyen TD, Xu H. A distributionally robust optimization approach for two-stage facility location problems. EURO J Comput Optim 2020;8(2):141–72.
[62] Cheng C, Adulyasak Y, Rousseau LM. Robust facility location under demand uncertainty and facility disruptions. Omega 2021;103:102429.
[63] Stienen V, Wagenaar J, den Hertog D, Fleuren H. Optimal depot locations for humanitarian logistics service providers using robust optimization. Omega 2021;104:102494.
[64] Snyder LV, Atan Z, Peng P, Rong Y, Schmitt AJ, Sinsoysal B. OR/MS models for supply chain disruptions: A review. IIE Trans 2016;48:89–109.
[65] Scaparra MP, Church RL. Location problems under disaster events. In: Laporte G, Nickel S, Saldanha da Gama F, editors. Location science. Springer, Cham.; 2019, p. 623–41.
[66] Dibene JC, Maldonado Y, Vera C, de Oliveira M, Trujillo L, Schütze O. Optimizing the location of ambulances in Tijuana, Mexico. Comput Biol Med 2017;80:107–15.
[67] Carson YM, Batta R. Locating an ambulance on the Amherst Campus of the State University of New York at Buffalo. Interfaces 1990;20:43–9.
[68] Moeini M, Jemai Z, Sahin E. Location and relocation problems in the context of the emergency medical service systems: A case study. CEJOR Cent Eur J Oper Res 2015;23:641–58.
[69] Bélanger V, Kergosien Y, Ruiz A, Soriano P. An empirical comparison of relocation strategies in real-time ambulance fleet management. Comput Ind Eng 2016;94:216–29.
[70] Aringhieri R, Carello G, Morale D. Ambulance location through optimization and simulation: the case of Milano urban area. Internal report, Dipartimento di Tecnologie dell'Informazione, Università di Milano; 2007.
[71] Aringhieri R, Carello G, Morale D. Supporting decision making to improve the performance of an Italian emergency medical service. Ann Oper Res 2016;236(1):131–48.
[72] Kahraman C, Topcu Y. Operations research applications in health care management. International series in operations research & management science, Springer; 2017.
[73] Vazirani VV. Approximation algorithms. Berlin, Heidelberg: Springer-Verlag; 2001.
[74] Frichi Y, Jawab F, Abouelji nane L, Boutahari S. Development and comparison of two new multi-period queueing reliability models using discrete-event simulation and a simulation–optimization approach. Comput Ind Eng 2022;168:108068.
[75] Schmid V, Doerner KF. Ambulance location and relocation problems with time-dependent travel times. European J Oper Res 2010;207(3):1293–303.
[76] Fadda E, Manerba D, Tadei R, Camurati P, Cabodi G. KPIs for Optimal Location of charging stations for Electric Vehicles: the Biella case-study. In: Ganzha M, Maciaszek L, Paprzycki M, editors. Proceedings of the 2019 federated conference on computer science and information systems. ACSIS, vol. 18, 2019, p. 123–6.
[77] Fadda E, Manerba D, Cabodi G, Camurati P, Tadei R. Evaluation of optimal charging station location for electric vehicles: An Italian case-study. In: Fidanova S, editor. Recent advances in computational optimization. Springer studies in computational intelligence, vol. 920, Springer; 2021, p. 71–87.
[78] Murray AT. Strategic analysis of public transport coverage. Socio-Econ Plan Sci 2001;35(3):175–88.

Edoardo Fadda is Assistant Professor of Operations Research at the Department of Mathematical Sciences "Luigi Lagrange", Politecnico di Torino, Italy. He received a Master Degree in Mathematical Engineering and the Ph.D. degree in Information Technology and System Engineering from the Politecnico di Torino, Italy, in 2014 and 2018, respectively. Since 2018 he is a member of the Isires (Istituto Italiano di Ricerca e Sviluppo) scientific and technical committee.

Daniele Manerba is Associate Professor of Operations Research at Università degli Studi di Brescia, Italy. He has been researcher at Politecnico di Torino (Italy) and at the Interuniversity Research Center on Enterprise Networks, Logistics and Transportation (CIRRELT) in Montréal, Canada. He holds a Ph.D. in Control and Information Engineering from Università degli Studi di Brescia, Italy. He is RU leader of the PRIN2020 project "ULTRAOPTYMAL" and has been leader of 2 WPs of the European H2020 project "SYNCHRO-NET". He is part of the Editorial Board of "Journal of Smart Cities and Society", "Journal of Optimization in Industrial Engineering" and "International Journal of Industrial Engineering and Production Research".

Roberto Tadei is an Emeritus Professor of Operations Research at Politecnico di Torino (Italy). Before retiring, his main research areas were in Combinatorial Optimization and in particular Transportation, Logistics, and Scheduling. He was author of more than 160 papers in international journals, conference proceedings, and monographs and co-inventor of two International Patents. He has been the President of the Italian Operations Research Society and the Italian Federation of Applied Mathematics.